NATIONAL AERONAUTICS AND SPACE ADMINISTRATION

Technical Report No. 32-852

Mariner-Mars Inertial Properties Determination and Midcourse Motor Alignment

W. W. Hough

J. D. Schmuecker

GPO PRICE $ _____

CFSTI PRICE(S) $ _____

Hard copy (HC) 3.00

Microfiche (MF) .65

ff 653 July 65

FACILITY FORM 602

N 68-25008 (ACCESSION NUMBER)

36 (PAGES)

CR 94666 (NASA CR OR TMX OR AD NUMBER)

(THRU) 1

(CODE) 30

(CATEGORY)

JET PROPULSION LABORATORY

CALIFORNIA INSTITUTE OF TECHNOLOGY

PASADENA, CALIFORNIA

May 15, 1968

NATIONAL AERONAUTICS AND SPACE ADMINISTRATION

Technical Report No. 32-852

Mariner-Mars Inertial Properties Determination and Midcourse Motor Alignment

W. W. Hough

J. D. Schmuecker

Approved by:

James N. Wilson, *Manager*
Mariner Spacecraft Development Section

JET PROPULSION LABORATORY
CALIFORNIA INSTITUTE OF TECHNOLOGY
PASADENA, CALIFORNIA

May 15, 1968

Copyright © 1968
Jet Propulsion Laboratory
California Institute of Technology

Prepared Under Contract No. NAS 7-100
National Aeronautics & Space Administration

CONTENTS

I. Introduction 1

A. Mission Description 1
B. Spacecraft Description 2
C. Prelaunch Operations 3
D. Flight Description 4
1. Launch Sequence 4
2. Trajectory Correction Sequence 4
3. Encounter Trajectory Accuracy 5

II. Coordinate Systems 5

A. Spacecraft Basic Reference (X-Y-Z) System 5
B. Pitch-Yaw-Roll (X′-Y′-Z′) System 5
C. Center-of-Gravity Measurement (u-v-w) System 5
D. Propulsion/Autopilot (a-b-c) System 9

III. Midcourse Motor Alignment 11

A. Substructure Description 11
B. Motor Adjustment Capability 12
1. Parameters 12
2. Allowable Center-of-Gravity Envelopes 14

IV. Analytical Weight and Center-of-Gravity Determination . . . 14

A. Description of Inertial Properties Computer Program 14
1. Program 14
2. Program Equations 14
B. Computer Program Utilization 16
C. Computer Program Accuracy 16

V. Experimental Weight and Center-of-Gravity Determination . . 17

A. Center-of-Gravity Test Hardware 17
B. Measurements of the Spacecraft Less the Propulsion System . . . 17
1. Weight and Center of Gravity in the Plane of Bay II 17
2. Center of Gravity Normal to the Plane of Bay II 19
C. Measurement of the Propulsion System 20
D. Calculation of Alignment Adjustments 20
E. Calculation of the Combined Center of Gravity 25

VI. Substructure Machining Operations 25

A. Substructure Machining Sequence 25
B. Spare Substructure Drill Fixture 26
1. General 26
2. Midcourse Maneuver Calculation Programs 29
C. Magnitude of Vernier Adjustments 29

Contents (contd)

VII. Method of Vernier Adjustments 26
A. Schematic Description 26
B. Vernier Adjustment Calculations 26

VIII. Accuracy 30
A. Velocity-Magnitude Errors 30
B. Pointing Errors 30
1. Center-of-Gravity Measurement Errors 30
2. Midcourse Motor-Alignment Errors 31
C. Effects on Total-Maneuver Execution Accuracy 31

IX. Discussion and Recommendations 31
A. Results of Interest 31
B. Recommendations 32

FIGURES

1. *Mariner* Mars Spacecraft 2
2. Midcourse motor-substructure assembly 3
3. Midcourse motor installed in the spacecraft 3
4. Spacecraft basic reference coordinate system 6
5. Mass centered pitch-yaw-roll coordinate system 7
6. Center-of-gravity measurement coordinate system 8
7. Propulsion/autopilot coordinate system 10
8. Midcourse motor installation 11
9. Midcourse motor substructure 12
10. Nominal midcourse configuration center-of-gravity envelope 13
11. Modification to nominal center-of-gravity envelopes by vernier-adjustment capability 13
12. Inertial properties computer program 15
13. Load cell installation 17
14. Spacecraft center-of-gravity test in plane of Bay II 18
15. Spacecraft-to-load cell adapter 18
16. Weights and reactions in center-of-gravity measurement 19
17. Spacecraft center-of-gravity test normal to plane of Bay II 19
18. Weights and reactions for determination of w_x 20
19. Propulsion system center-of-gravity test in plane of Bay II 20
20. Propulsion system center-of-gravity test normal to plane of Bay II . . . 21
21. Horizontal alignment of thrust vector and combined center of gravity . . 22
22. Vertical alignment of thrust vector and combined center of gravity . . . 23
23. Spare substructure drill jig 24
24. Midcourse maneuver schematic 27
25. Stabilized thrust vector 27

ABSTRACT

The mass of a spacecraft whose mission requires a precise trajectory must be accurately known for booster performance calculations and for burn-time calculations associated with on-board rocket engine firings. The position of the center of gravity (cg) of a spacecraft must be accurately known so that the thrust vector of the on-board propulsion system may be aligned to eliminate offset torques during motor firing. If perfect alignment of the thrust vector to the cg is not accomplished, maneuver events may be modified to correct for the misalignment, but only if the misalignment is known.

The application of these requirements to the *Mariner* Mars *1964* fly-by mission is the subject of this Report. The method of analytically and experimentally determining the weight and cg of *Mariner* Mars and of positioning its midcourse motor are discussed in detail. Particular attention is paid to the method of vernier adjustments on maneuver turns to account for known misalignment of the nominal thrust vector to the cg. The effect of the tolerances involved in weight and cg measurement and in motor positioning on total midcourse maneuver accuracy is also discussed. Recommendations for future programs are offered.

I. INTRODUCTION

This Report covers the inertial property determination and alignment of the midcourse motor for the *Mariner*-Mars 1964 spacecraft. The midcourse motor was fired several days after launch to provide accurate post-injection corrections to the trajectory.

Requirements for achieving satisfactory maneuver accuracy were that cg location, mass, and motor alignment be determined within specified tolerances. During the program, a method was found to correct for known motor thrust axis-cg misalignments by biasing the midcourse maneuver turns.

The position of the cg had to be controlled, from the beginning of the program, so that it was compatible with the alignment and correction capability constraints. Additionally, the weight had to be controlled so that it was within the boost capability of the launch vehicle. The spacecraft moment of inertia had to be predicted to properly size elements of the attitude control system. This Report describes the approach taken to satisfy the above requirements.

A. Mission Description

When the *Mariner* Mars spacecraft passed Mars in mid-July, 1965, equipment aboard the spacecraft took 21 photographs of the Martian surface. The Martian atmospheric pressure was measured by occultation of the radio signals

from the spacecraft as it passed behind the planet. During its 8½ mo journey, the spacecraft measured radiation, magnetic fields, and micrometeorite densities in space. In addition, the spacecraft returned quantities of engineering data, such as temperatures, starlight intensities, gas pressures, and rotational rates. The communications distance to Earth during the post-encounter period was approximately 190 million mi. *Mariner IV (Mariner* Mars 1964) followed the unsuccessful launch of an identical spacecraft, *Mariner III*. A third flight vehicle was provided as a spare.

B. Spacecraft Description

A photograph of the *Mariner* Mars *1964* spacecraft is shown in Fig. 1. The basic structure of *Mariner* Mars was an octagonal machined frame to which all spacecraft items were mounted. There were eight rectangular bay openings around the periphery of the structure. Seven of the bays contained electronic equipment. The 50-lb thrust monopropellant restartable midcourse motor was housed in the eighth bay. The midcourse propulsion system was positioned in this bay so that its thrust axis was approximately normal to the roll axis of the spacecraft. It was mounted to the basic structure by means of an adjustable substructure. Figure 2 shows the substructure mounted to the midcourse motor, and Fig. 3 the method used in mounting the assembly to the spacecraft. Previous JPL spacecraft designs pointed the midcourse thrust vector parallel to the axis of symmetry of the structure. This design was changed in *Mariner* Mars for three reasons:

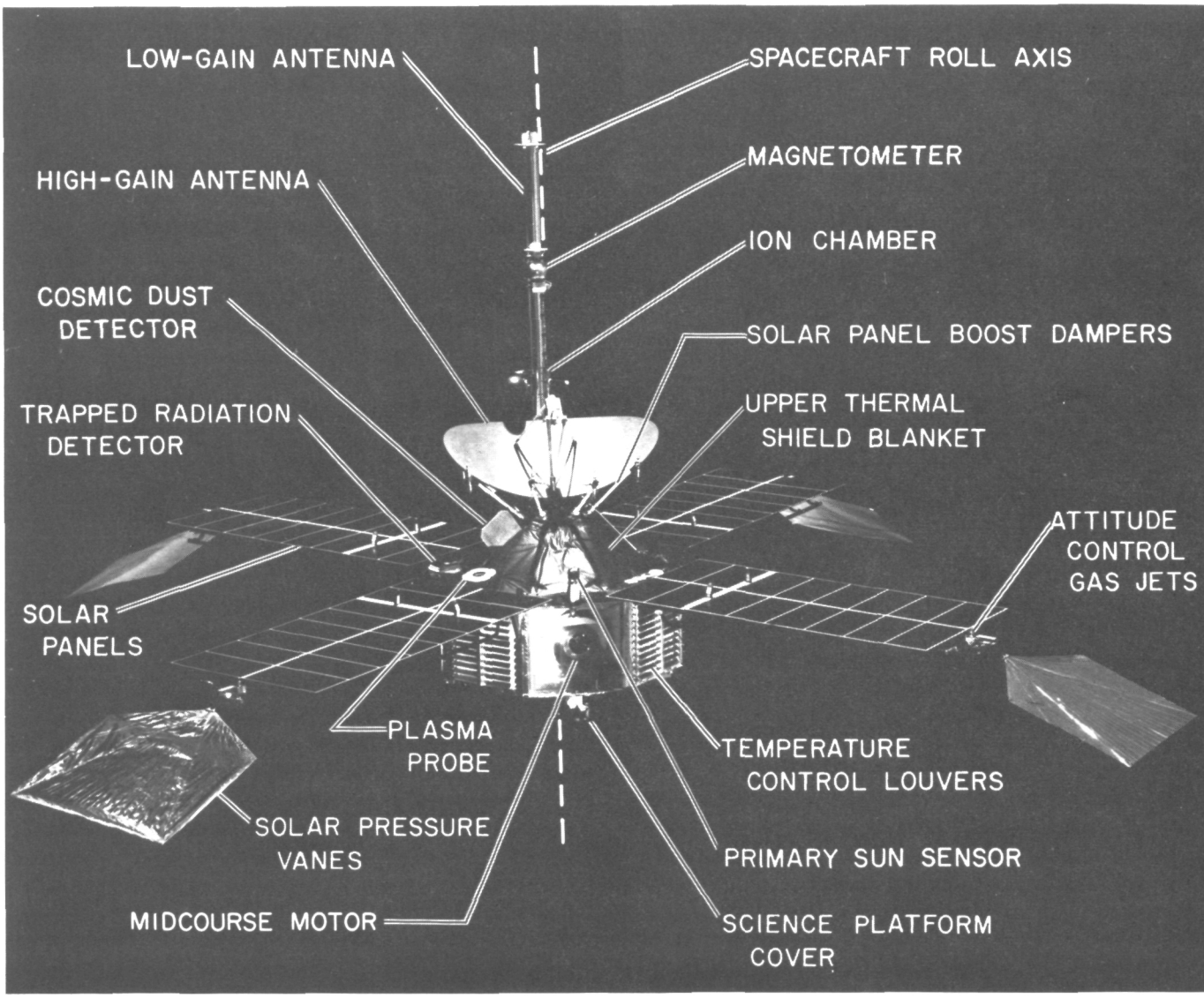


Fig. 1. *Mariner-Mars* Spacecraft

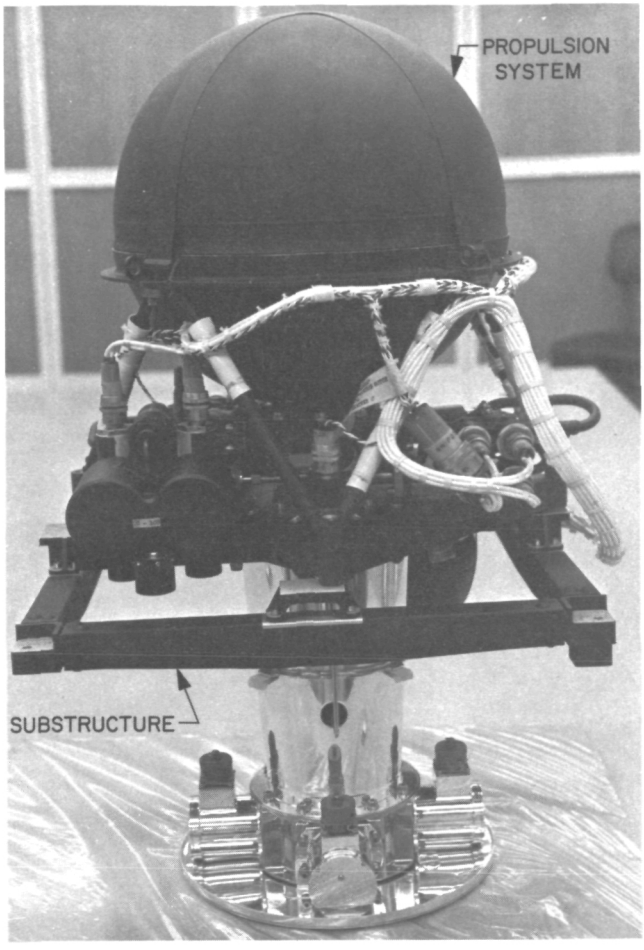


Fig. 2. Midcourse motor-substructure assembly

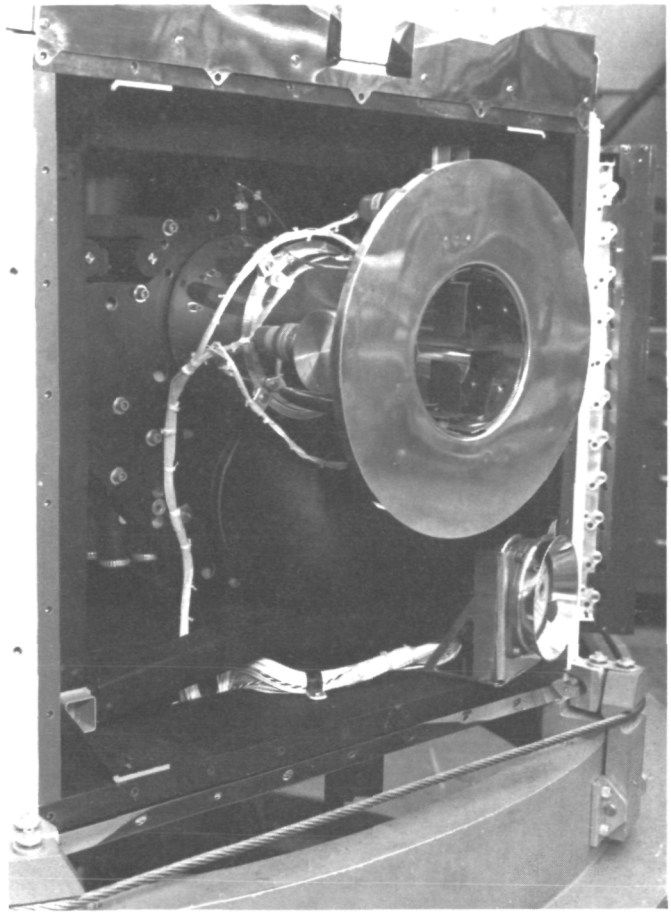


Fig. 3. Midcourse motor installed in the spacecraft

1. An early requirement to have the option of performing a maneuver without changing the solar panel orientation with respect to the Sun. Trajectory correction maneuvers requiring roll turns of ± 180 deg could have been performed without decreasing the electrical output of the solar panels.
2. The requirement from Mars encounter geometry for positioning the planetary experiments beneath the structure in the traditional motor location.
3. More favorable antenna pointing geometry during the midcourse maneuver eliminating the need for an additional antenna.

Four solar panels were deployed from their folded position after the boost phase into a plane perpendicular to the Sun line. High gain and low gain antennas were mounted atop the spacecraft. Full attitude stabilization was required to keep the solar panels facing the Sun and the fixed high gain antenna pointed at Earth. Attitude control was maintained by 12 nitrogen gas jets and four solar pressure vanes mounted at the tips of the solar panels. Attitude reference was provided by sensors which tracked the Sun and the star Canopus. Three gyros were provided for attitude control during maneuvers and in the event of loss of Sun and star references. Spacecraft temperatures were controlled by painted and polished surfaces, thermal shields, and thermally actuated louvers. Scientific instruments were mounted on the low gain antenna and on the basic structure. The television camera was mounted on a rotating platform beneath the spacecraft.

C. Prelaunch Operations

During the development of *Mariner* Mars, constant analytical determinations of the weight, cg, moments of inertia and products of inertia were made. The cg predictions were used to assure that the final cg would be within the motor adjustment capability. When the flight spacecrafts were assembled, experimental measurements of their weights and cg positions were made. These measurements yielded a much higher degree of accuracy than the analytical predictions. The propulsion subsystem was

positioned after the experimental cg determination was made. Just prior to the flight at the Eastern Test Range (ETR), the weight and cg were again measured. If the cg-shifts caused by hardware replacements had been greater than the vernier adjustment capability, it would have been necessary to reposition the propulsion subsystem.

D. Flight Description

1. Launch Sequence

The *Mariners* were launched by *Atlas-Agena D* boost vehicles. Just after injection into the interplanetary trajectory, the spacecraft was separated from the *Agena* second stage. This occurred with the spacecraft still in the boost configuration. The solar panels were still folded approximately parallel to the roll axis. Relative velocity at separation was imparted to the spacecraft by four mechanical spring mechanisms symmetrically mounted on the *Agena*-spacecraft adapter. To minimize rotational rates at separation, it was necessary to control the configuration of the spacecraft so that the cg would be near the roll axis. Tip-off rates less than 3 deg/sec were required, with rates less than 1 deg/sec desired. This constraint required that the spacecraft cg envelope in the boost configuration be a 2.25-in. D cylinder centered about the roll axis.

2. Trajectory Correction Sequence

a. General. Based on tracking data from the first few days of flight, several trajectory correction maneuvers were calculated that would change the velocity vector of the spacecraft to bring it into the proper Mars encounter zone at a predetermined time. Those maneuvers that were outside the capability of the propulsion system, or in which turns violated constraints imposed by thermal control or antenna patterns, were discarded.

The average position of the cg during maneuver was predicted by modifying the position of the cg determined at the last cg test, accounting for estimated cg shifts in flight and estimating the amount of fuel to be used during motor burn.[1] The average orientation of the final thrust vector was then determined within the frame of reference of the spacecraft. It is this average stabilized thrust vector that was positioned in inertial space during motor burn.

With the best maneuver chosen, commands for pitch and roll turn durations and polarities, and propulsion system burn duration were sent and stored in the Central Computer and Sequencer (CC&S) of the spacecraft. The maneuver sequence was controlled by the CC&S, which also had direct control of attitude stabilization logic functions during the maneuver. The sequence was initiated by turning on the gyros for warm-up. After 1 hr, the attitude reference was switched to the gyros from the Sun and Canopus sensors. A pitch turn and then a roll turn were made using the known precessional rate of the gyros as reference. The position error signal of the gyros was followed by the spacecraft, its attitude being changed by the gas jets for the commanded time duration. When the turns were completed, the proper maneuver attitude was maintained by the gas jet system using the gyros as position references.

During motor firing, the autopilot maintained the inertial orientation of the spacecraft. Its function was to control the direction of the thrust vector by means of four jet vanes located in the motor's exhaust stream, Fig. 3. The autopilot converted the position error signals from the gyros into appropriate position commands for the jet vanes. The jet vanes rotated the thrust vector so that the thrust vector passed through the spacecraft cg. Following motor burn, inertially referenced attitude was maintained by the gas jets until the CC&S released control and the normal acquisition logic accomplished reacquisition of the celestial references.

b. Method of vernier thrust axis adjustment. The autopilot had the capability of pointing the actual stabilized motor thrust vector through the cg if the angle between it and the undeflected thrust vector (intersection at the jet vane center of lift) was less than 20 milliradians (mrad). The less the misalignment, however, the better the accuracy. The mounting of the propulsion system to the spacecraft included adjustments so that nominally perfect alignment could be accomplished. If after motor positioning the cg shifted due to prelaunch component replacement or abnormal performance of articulating parts in flight, correction to the maneuver could be made for the misalignment. This correction method is called the method of vernier adjustment.

Instead of pointing the motor center line in the direction of the desired velocity increments, vernier adjustments could be made on maneuver pitch and roll turns. These turns would orient the *Mariner* so that after rotations due to initial offset torques, the average stabilized thrust vector would be pointed in the required direction.

3. Encounter Trajectory Accuracy

The extreme preciseness required from the midcourse maneuver and attained in the *Mariner* Mars trajectory is

[1]The fuel consumption caused a slight cg shift during the maneuver.

illustrated by the following brief description of encounter parameters:

Mariner Mars had traveled 325 million mi at encounter. Before the midcourse maneuver, it would have missed the Mars aiming zone by 160,000 mi. An aiming point to optimally perform the planetary experiments was chosen prior to the maneuver. This point was 7,450 mi from the center of the planet and was defined in a plane perpendicular to the aerocentric (Mars-centered) approach asymptote of the spacecraft. *Mariner* Mars missed the nominal aiming point by only 1,770 mi, well within the zone necessary to obtain television and occultation data.

II. COORDINATE SYSTEMS

Four spacecraft-centered coordinate systems were used. Each one was separately useful in analytically and experimentally determining the cg, performing maneuver calculations, and determining the rotation of the flight spacecraft at motor ignition.

A. Spacecraft Basic Reference (X-Y-Z) System

The basic reference (*X*-*Y*-*Z*) system was used for cg calculations and is shown in Fig. 4. Octagon corner-and-bay labeling are shown in the diagram. The eight corners of the *Mariner* Mars octagon were labeled *A* through *H*. The eight sides (bays) were labeled I through VIII. Both are read in a clockwise direction when viewed from above (Sun side of the spacecraft). Bay I was between corners *A* and *B*.

1. Origin: The center of the octagon structure, Point Q, in the plane formed by the spacecraft-booster mating surfaces at the base of the eight corners. (This plane was the separation plane.)
2. *X* axis: In the separation plane and passing positively through the nominal center of Bay I between corners *A* and *B*.
3. *Y* axis: In the separation plane, normal to *X*, and passing positively through the nominal center of Bay III between corners *C* and *D*.
4. *Z* axis: Normal to the separation plane and positive aft (anti-Sun direction).

B. Pitch-Yaw-Roll (X′-Y′-Z′) System

The pitch-yaw-roll system was used in the calculations that determined the midcourse maneuver parameters. Moments and products of inertia and rotational rates and positions were calculated and measured about the pitch-yaw-roll axes shown in Fig. 5.

1. Origin: The center of gravity of the spacecraft, Point S.
2. X' or pitch axis: Parallel to and in the same direction as the X axis.
3. Y' or yaw axis: Parallel to and in the same direction as the Y axis.
4. Z' or roll axis: Parallel to and in the same direction as the Z axis.

Since the pitch-yaw-roll system evolved from the reference coordinate system by translation of the respective reference cg coordinates, the following transformation can be written:

$$\begin{Bmatrix} X' \\ Y' \\ Z' \end{Bmatrix} = \begin{Bmatrix} X - \overline{X} \\ Y - \overline{Y} \\ Z - \overline{Z} \end{Bmatrix} \tag{1}$$

where, for example, $\overline{X}$ denotes the location of the cg along the X axis.

C. Center-of-Gravity Measurement (u-v-w) System

The midcourse motor was mounted to Bay II by the substructure that mounted, in turn, to four mounting brackets whose mounting surfaces were parallel to the bay face. The motor substructure had four corresponding pads at the corners. The motor assembly was installed in the spacecraft by fastening four bolts through each substructure pad into the octagon mounting brackets.

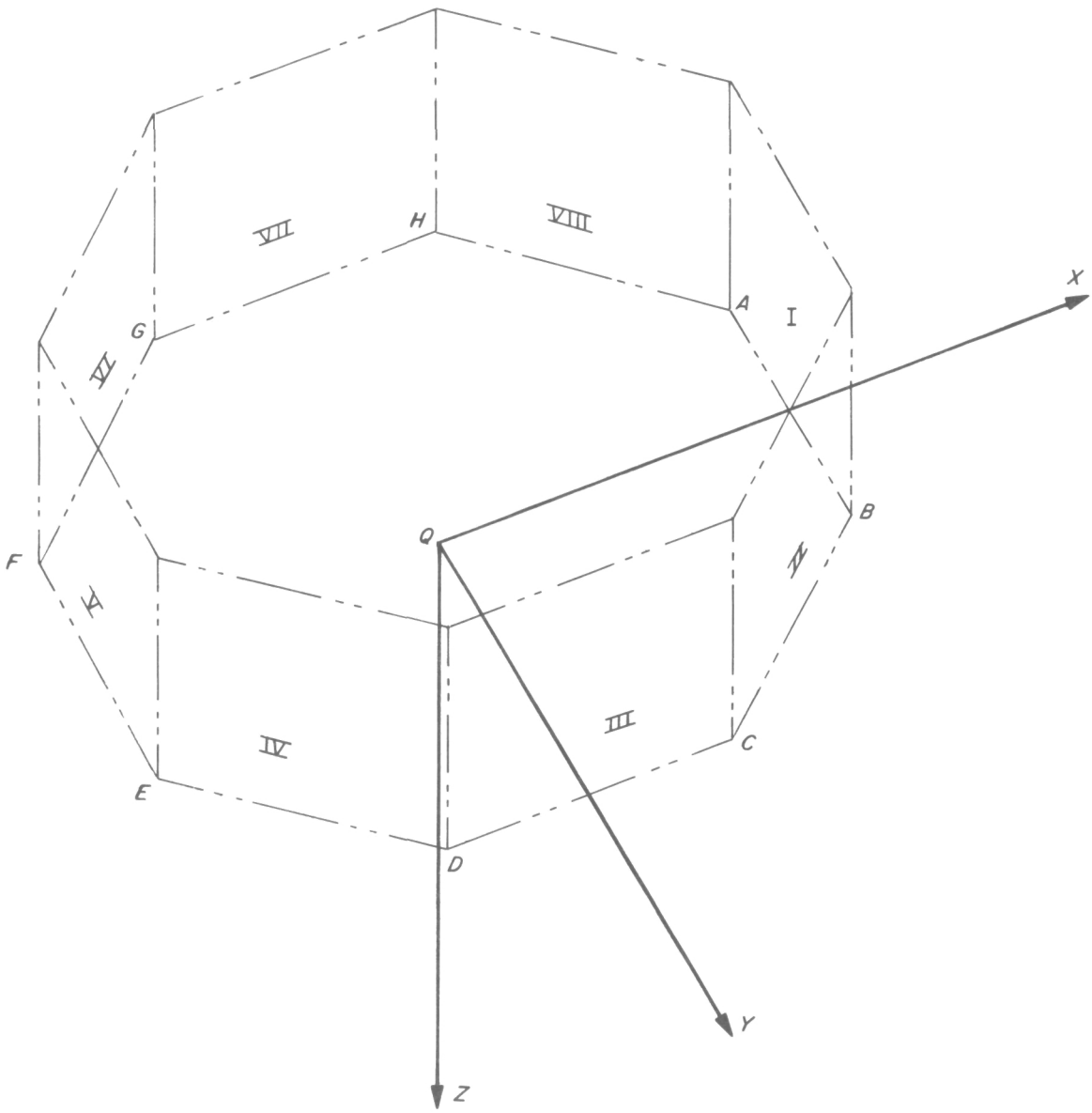


Fig. 4. Spacecraft basic reference coordinate system

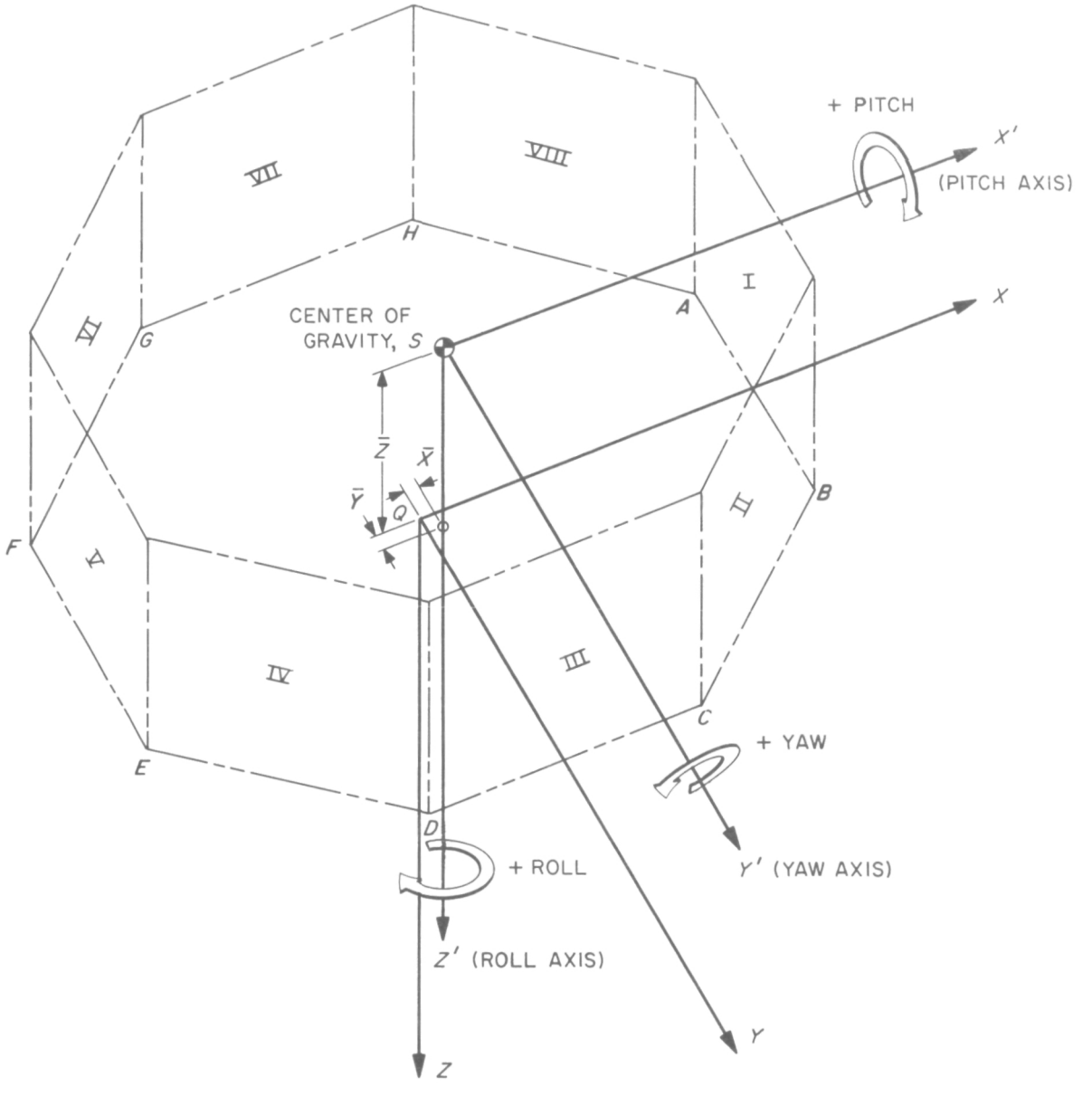


Fig. 5. Mass centered pitch-yaw-roll coordinate system

To eliminate tolerance buildups between the motor substructure/octagon interface plane and other references, the cg was experimentally measured directly from this plane. The u-v-w coordinate system, as shown in Fig. 6, was defined as follows:

1. Origin: The intersection of the substructure/octagon mating plane and the center of the lower mounting bolt hole closest to Corner C. This point is termed P in Fig. 6.
2. u axis: In the mating plane, parallel to the Z axis, and positive forward.
3. v axis: In the mating plane, perpendicular to the u axis and positive toward Corner B.
4. w axis: The third axis of this right-handed system, normal to the mating plane and positive inboard.

The coordinates of point P *in the* X-Y-Z system given in the figure were actual spacecraft fixed dimensions in inches.

$$\begin{Bmatrix} X_P \\ Y_P \\ Z_P \end{Bmatrix} = \begin{Bmatrix} 9.924 \\ 20.130 \\ -1.502 \end{Bmatrix} \tag{2}$$

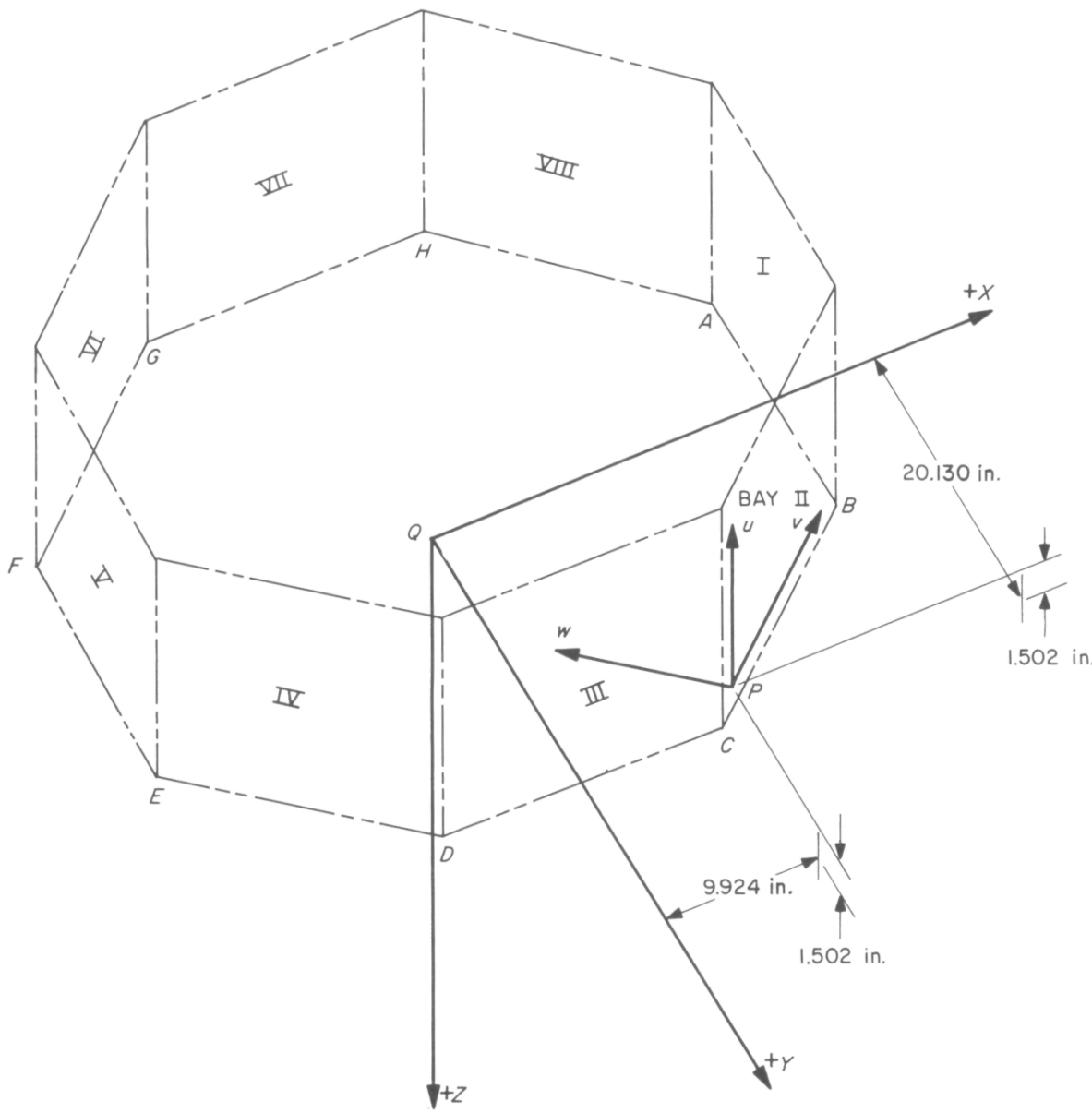


Fig. 6. Center-of-gravity measurement coordinate system

The direction cosines between the u-v-w system and the X-Y-Z system are:

	X	Y	Z
u	0	0	-1
v	$\cos 45$ deg	$-\cos 45$ deg	0
w	$-\cos 45$ deg	$-\cos 45$ deg	0

Calling the matrix of these direction cosines $[R]$, the transformation from X-Y-Z to u-v-w is written:

$$\begin{Bmatrix} u \\ v \\ w \end{Bmatrix} = [R] \begin{Bmatrix} X - X_P \\ Y - Y_P \\ Z - Z_P \end{Bmatrix} \tag{3}$$

Since a matrix of direction cosines is orthonormal, the inverse is equal to the transpose or:

$$[R]^{-1} = [R]^T \tag{4}$$

Thus the transformation from u-v-w to X-Y-Z can be written as:

$$\begin{Bmatrix} X \\ Y \\ Z \end{Bmatrix} = [R]^T \begin{Bmatrix} u \\ v \\ w \end{Bmatrix} + \begin{Bmatrix} X_P \\ Y_P \\ Z_P \end{Bmatrix} \tag{5}$$

D. Propulsion/Autopilot (a-b-c) System

The function of the autopilot was to control spacecraft attitude during the midcourse motor burn by rotating the jet vanes to eliminate offset torques. It was convenient to use a coordinate system for autopilot performance predictions that was based on jet vane orientation. This a-b-c coordinate system is shown in Fig. 7 along with the pitch-yaw-roll system described in Section IIB. The a-b-c system was used for vernier adjustment calculations.

1. Origin: The intersection of the rocket motor center line, which was the nominal undeflected thrust axis, and a line perpendicular to this center line that passed through the spacecraft center of gravity, Point S. This origin is labeled Point 0 in Fig. 7.
2. a axis: Along the nominal motor center line, positive in the direction of gas exhaust, or Bay II.
3. b axis: Parallel to the X-Y (or X'-Y') plane, positive toward Bay IV.
4. c axis: The third orthogonal right-handed axis, thus positive aft.

The undeflected thrust vector, or nominal motor center line, made the polar angles of γ to the X' axis in the X'-Y' plane and of ξ to the Z' axis. These angles were fixed by midcourse motor angular positioning. In Fig. 7, γ is shown to line SL and ξ to line SN. SN is parallel to the a axis, but offset by the misalignment between the undeflected thrust axis and the center of gravity. This misalignment is illustrated in the figure by $\bar{b}$ and $\bar{c}$, the coordinates of the cg in the a-b-c system. $\bar{a} = 0$ by the definition of the origin of this coordinate system.

The direction cosines between the X'-Y'-Z' and a-b-c coordinate systems are:

	X'	Y'	Z'
a	$\cos\gamma \sin\xi$	$\sin\gamma \sin\xi$	$\cos\xi$
b	$-\sin\gamma$	$\cos\gamma$	0
c	$-\cos\gamma \cos\xi$	$-\sin\gamma \cos\xi$	$\sin\xi$

Calling the matrix of these direction cosines L, the transformation from X'-Y'-Z' to a-b-c can be written:

$$\begin{Bmatrix} a \\ b \\ c \end{Bmatrix} = [L] \begin{Bmatrix} X' - X'_0 \\ Y' - Y'_0 \\ Z' - Z'_0 \end{Bmatrix} \tag{6}$$

where, for example, X'_0 denotes the X' coordinate of Point 0, the origin of the a-b-c system. Since a matrix of direction cosines is orthonormal,

$$[L]^{-1} = [L]^T \tag{7}$$

The transformation from a-b-c to X'-Y'-Z' can be given as:

$$\begin{Bmatrix} X' \\ Y' \\ Z' \end{Bmatrix} = [L]^T \begin{Bmatrix} a \\ b - \bar{b} \\ c - \bar{c} \end{Bmatrix} \tag{8}$$

To related Point 0 to Point S in either system, Eq. 6 can be used:

$$\begin{Bmatrix} \bar{a} \\ \bar{b} \\ \bar{c} \end{Bmatrix} = [L] \begin{Bmatrix} X'_0 \\ Y'_0 \\ Z'_0 \end{Bmatrix} = \begin{Bmatrix} 0 \\ \bar{b} \\ \bar{c} \end{Bmatrix} \tag{9}$$

or Eq. (8):

$$\begin{Bmatrix} X'_0 \\ Y'_0 \\ Z'_0 \end{Bmatrix} = [L]^T \begin{Bmatrix} 0 \\ \bar{b} \\ \bar{c} \end{Bmatrix} \tag{10}$$

Useful transformations from the autopilot system to the basic reference system can also be developed by the substitution of Eq. (1) in (6) or (8).

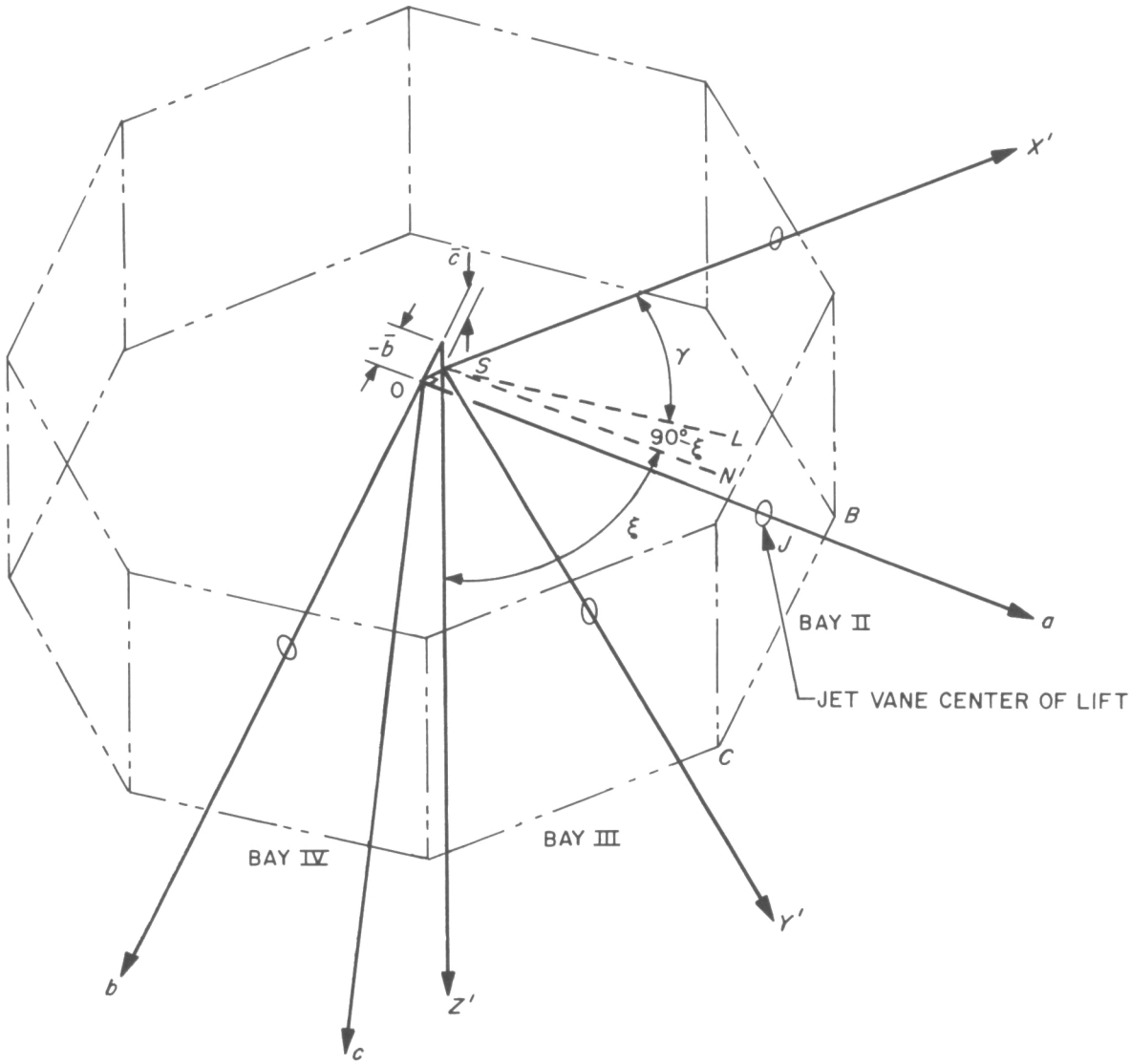


Fig. 7. Propulsion/autopilot coordinate system

III. MIDCOURSE MOTOR ALIGNMENT

The midcourse motor was mounted to the spacecraft by a substructure. The functions of the substructure were to: (1) provide sufficient structural support for the motor, and (2) adjust the thrust axis of the motor so it passed through the spacecraft cg. The substructure and its associated adjustment capability described in this Report is a second generation design. The earlier design was discarded because its motor adjustment capability was too restrictive and did not take advantage of all the available space. An assembly schematic of the midcourse motor installation is shown in Fig. 8. Figure 9 is a detail of the second generation flight substructure.

A. Substructure Description

The substructure was fabricated of four square aluminum tubes, shown in Fig. 2. The four corner joints were made by fittings that also provided the substructure-to-spacecraft mounting surface. This plane, shown as plane *B* in Fig. 8 and 9, contained axes *u* and *v* as described in Section IIC. The holes in the four fittings accepted close tolerance bolts that attached the substructure to the four brackets on the spacecraft. The mounting planes of these brackets were parallel to Bay II. In the approximate centers of the square tubes, four midcourse motor mounting

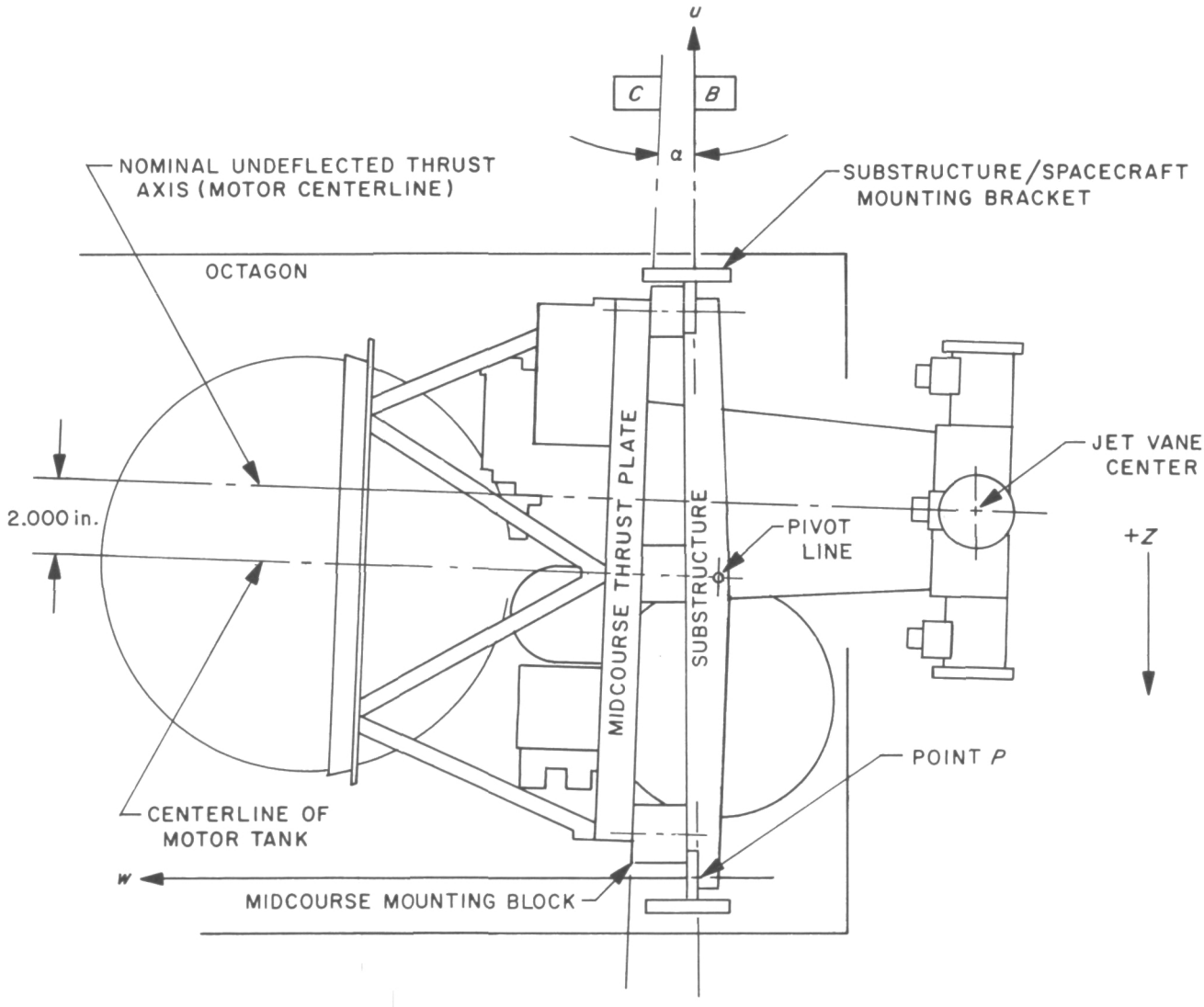


Fig. 8. Midcourse motor installation

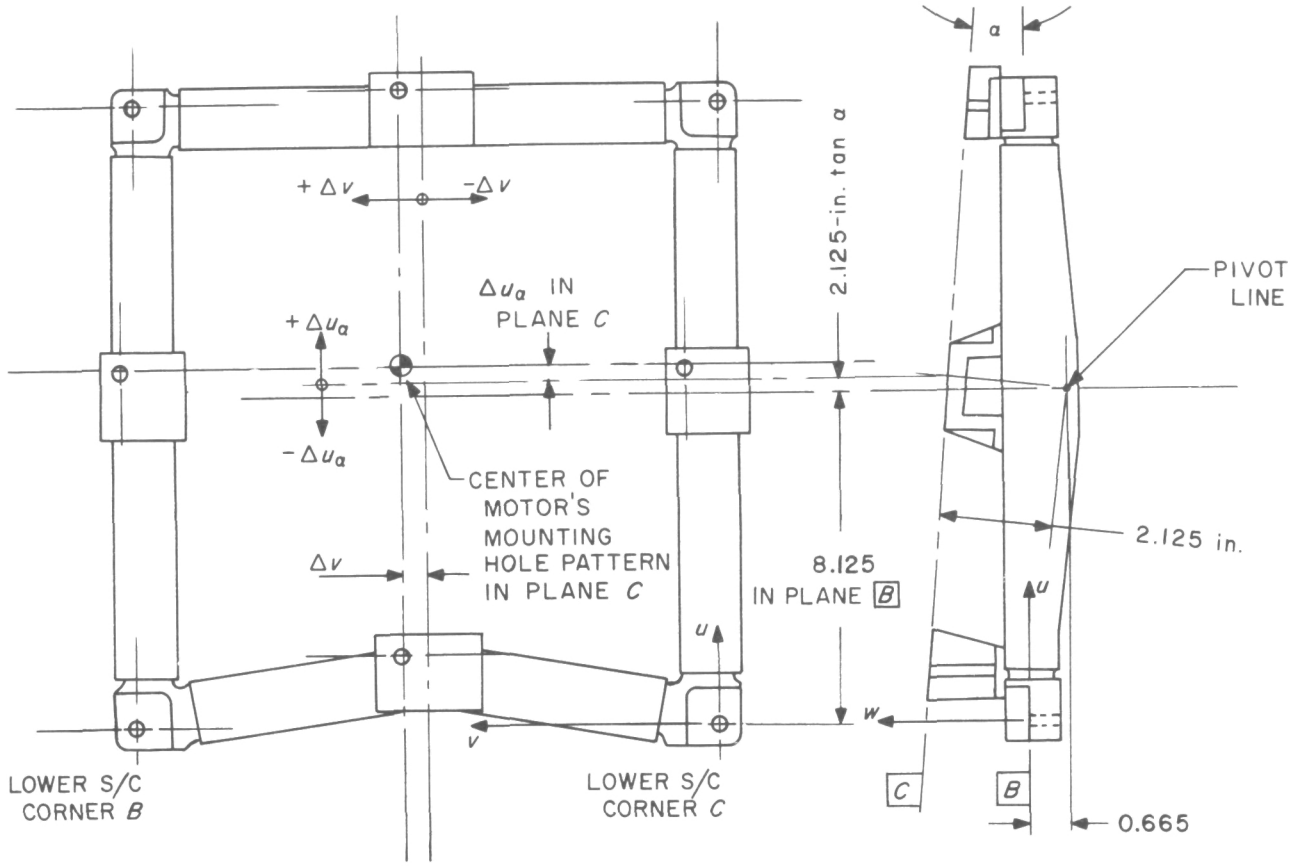


Fig. 9. Midcourse motor substructure

blocks were mounted. The tops of these blocks, approximately 1.5 in. square, were machined coplanar and to the proper angle α after assembly. This plane is shown as plane C in Fig. 8 and 9. The midcourse motor thrust plate was mounted to this plane by close tolerance bolts, one at each of the four blocks. The relationship between the hole pattern that was machined in these blocks for the motor and the substructure/spacecraft mounting hole pattern was established after the cg had been determined.

B. Motor Adjustment Capability

1. Parameters

After the cg measurement, three variable parameters were specified and used in the machining of the substructure's mounting blocks. These parameters were adjusted to align the nominal thrust axis of the motor (its center line) to the cg. Before describing the three adjustments, discussion of two constraints is appropriate:

1. The projection of the thrust axis in the X-Y plane was perpendicular to the plane of Bay II. In other words, the polar angle γ, described in Section IID, was fixed at 45 deg.
2. There existed a defined reference line, called the pivot line, that fixed the relationship between the motor and the spacecraft. This pivot line had been defined in the earlier design, and was retained to minimize changes to other spacecraft subsystems. The pivot point was in Bay II, 21.916 in. from the Z axis as measured 45 deg to the X axis. Its Z coordinate was -9.625 in.

The three adjustments that could be made to align the thrust axis of the motor with the cg were:

1. A rotation of plane C about the pivot line so that it made an angle to plane B of $\alpha = 0$ deg to $\alpha = 4$ deg. In other words, the polar angle ξ described in Section IID was variable between 86 and 90 deg.
2. A horizontal translation of the mounting hole pattern of the motor in plane C by as much as 0.500 in. either way from the center of Bay II parallel to the X-Y plane, or along the v axis. This translation is shown by Δv in Fig. 9.

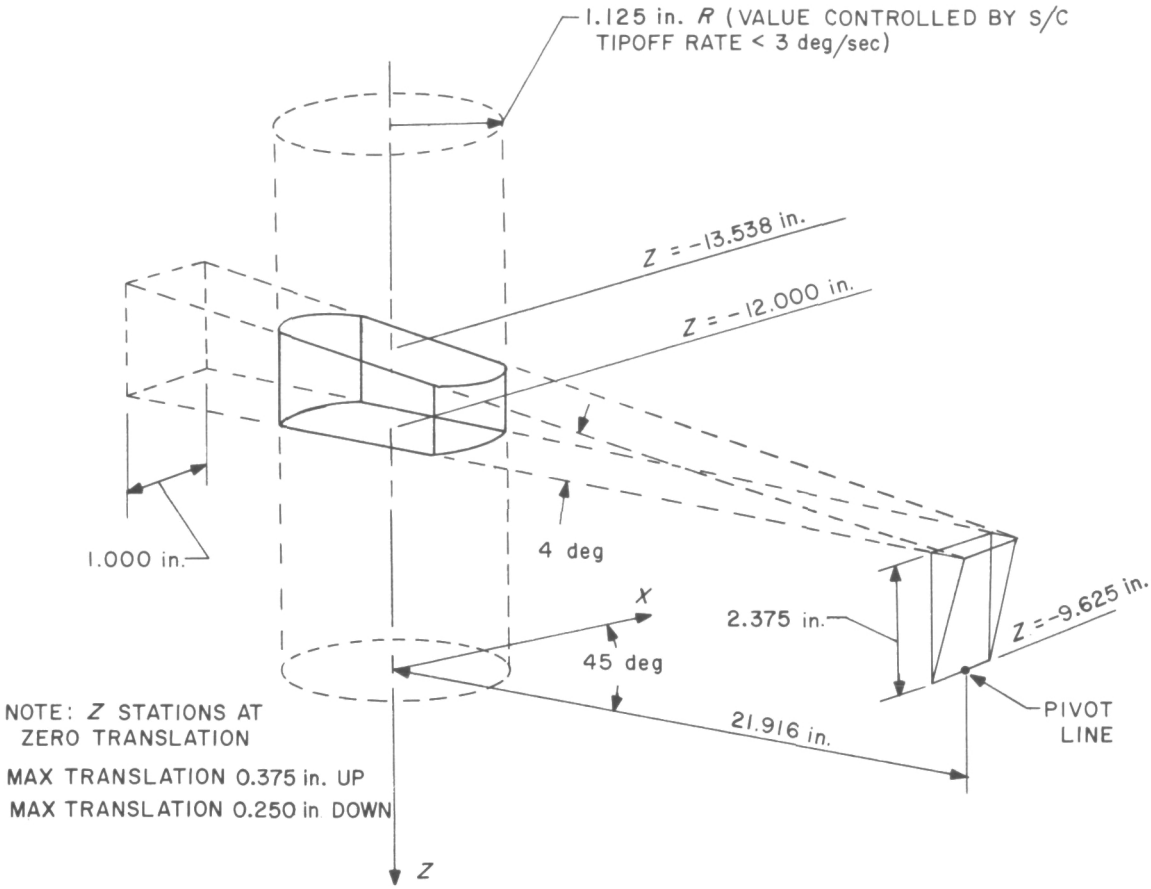


Fig. 10. Nominal midcourse configuration center-of-gravity envelope

3. A vertical translation of the motor's mounting hole pattern in plane C by as much as 0.375 in. up and as much as 0.25 in. down. This translation is shown by Δu_α in Fig. 9. The dimension Δu_α is parallel to the c axis defined in Section IID. With $\Delta u_\alpha = 0$, the center line of the motor tank would pass through the pivot line as shown in Fig. 8.

Because of clearance requirements between the motor assembly hardware and the spacecraft, there were limitations on the allowable translations as a function of Δu_α and α. The 0.375 in. upward translation was available for all angles. For angles of α between 1 and 4 deg, ample downward translation could be provided. However, for angles less than 1 deg, vertical translation was restricted. The approximate vertical translational adjustment was redundant to the rotational adjustment for the majority of cg positions. The adjustment was included to allow each of the midcourse motors for the three flight spacecraft to be positioned at the same angle. This was desirable because

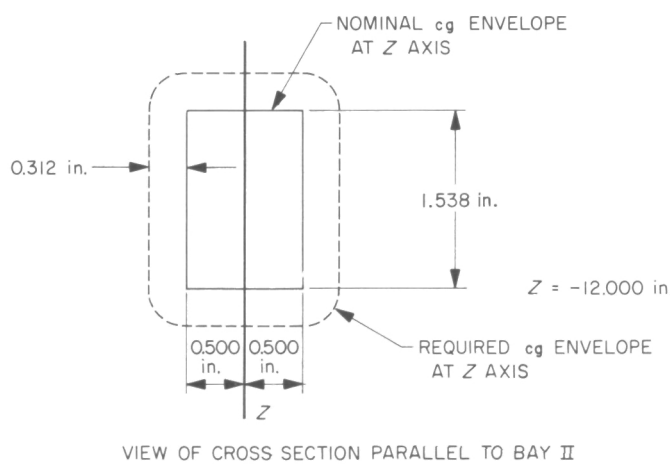


Fig. 11. Modification to nominal center-of-gravity envelopes by vernier-adjustment capability

each autopilot had to be calibrated for the angular rotation. The use of identical angles allowed for autopilot interchangeability.

2. Allowable Center-of-Gravity Envelopes

The adjustment capability of the midcourse motor mounting hardware and the associated positioning constraints defined a prismatic corridor that nominally contained the spacecraft midcourse configuration cg. The cg envelope required for launch, bounded this corridor because the X and Y coordinates of the cg did not change appreciably from launch to cruise configuration. This was because the solar panels and solar vanes were symmetric about the Z axis. To ensure that vibratory interference problems between the motor and the spacecraft were eliminated, the base of the allowable cg corridor was taken at the lowest point that would allow dynamic clearance along the 1-in. lateral adjustment range with no rotation. This cg envelope, which allowed perfect alignment of the nominal thrust axis with the cg, is shown in Fig. 10.

The required cg envelope was larger than the corridor shown in Fig. 10 by the amount of vernier adjustment capability. This capability was 0.312 in. offset at the Z axis. Figure 11, a cross-section through the envelope at the Z axis, shows the maximum allowable cg envelope for midcourse maneuver.

IV. ANALYTICAL WEIGHT AND CENTER-OF-GRAVITY DETERMINATION

During the development phase of a spacecraft program, predictions of the flight weight and cg position are necessary. Weight control must be maintained so that the capability of the launch vehicle is not exceeded. Control over the cg must be maintained if it is to fall within the required boost or midcourse envelope. Therefore, before an actual spacecraft is available for measurement, an analytical method of determining weight and cg is required. During the development of *Mariner* Mars, this requirement was satisfied by the Inertial Properties Computer Program (IPCP).

A. Description of Inertial Properties Computer Program

1. Program

The IPCP, Fig. 12, was used to calculate weight, cg, centroidal moments of inertia, and products of inertia about the pitch, yaw, and roll axes. The item designation, weight, position coordinates in the basic reference system, local moments of inertia, and local products of inertia for each component were given as inputs to an IBM 7094 computer program. Components were idealized as simple shapes so that local moments of inertia could be easily hand-calculated. Local products of inertia of a component are other than zero only when the orientation of the simple shape is such that its principal axes are not parallel to the basic reference system. Component inertial parameters were input to the computer by groups, for example: basic structure, propulsion system, electronics in each octagonal bay, scientific experiments, attitude control system, solar panels, etc. The computer found the inertial properties of each group and listed these subtotals before it computed and listed the totals for the composite spacecraft. Computer runs were made for each spacecraft configuration: launch, cruise, and encounter.

The listing by groups was an extremely valuable procedure. If a computer run showed that the composite weight or cg position was outside the requirement for these properties, the subsystem that caused the violation could be immediately located by the group subtotals and appropriate correction made in the design to bring the property back in tolerance. A complete computer printout containing a listing of all inputs, became an excellent hardware list and provided a bookkeeping record for all future changes.

2. Program Equations

The defining equations used by the computer to compute inertial properties were:

Weight:

$$W_G = \sum_{i=1}^{n} W_i \tag{11}$$

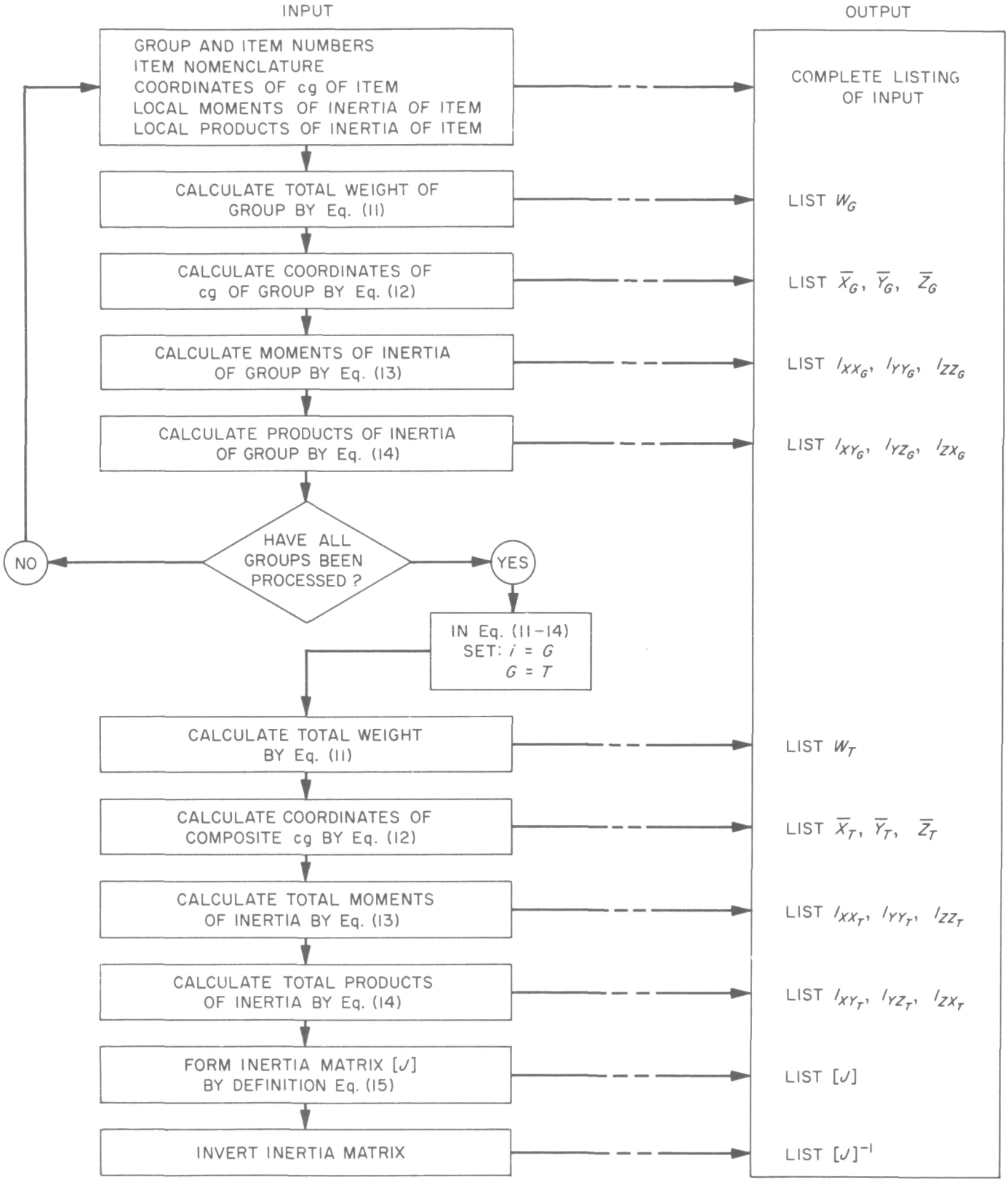


Fig. 12. Inertial properties computer program

Coordinates of the center of gravity

$$\overline{X}_G = \frac{\sum_{i=1}^{n} X_i W_i}{W_G}$$

$$\overline{Y}_G = \frac{\sum_{i=1}^{n} Y_i W_i}{W_G} \qquad (12)$$

$$\overline{Z}_G = \frac{\sum_{i=1}^{n} Z_i W_i}{W_G}$$

Centroidal moments of inertia:

$$I_{xx_G} = \sum_{i=1}^{n} W_i \left[(Y_i - \overline{Y}_G)^2 + (Z_i - \overline{Z}_G)^2\right] + I_{xx_i}$$

$$I_{yy_G} = \sum_{i=1}^{n} W_i \left[(Z_i - \overline{Z}_G)^2 + (X_i - \overline{X}_G)^2\right] + I_{yy_i} \qquad (13)$$

$$I_{zz_G} = \sum_{i=1}^{n} W_i \left[(X_i - \overline{X}_G)^2 + (Y_i - \overline{Y}_G)^2\right] + I_{zz_i}$$

Centroidal products of inertia:

$$I_{xy_G} = \sum_{i=1}^{n} W_i \left[(X_i - \overline{X}_G)(Y_i - \overline{Y}_G)\right] + I_{xy_i}$$

$$I_{yz_G} = \sum_{i=1}^{n} W_i \left[(Y_i - \overline{Y}_G)(Z_i - \overline{Z}_G)\right] + I_{yz_i} \qquad (14)$$

$$I_{zx_G} = \sum_{i=1}^{n} W_i \left[(Z_i - \overline{Z}_G)(X_i - \overline{X}_G)\right] + I_{zx_i}$$

Inertia matrix:

$$[J] = \begin{bmatrix} I_{xx} & -I_{xy} & -I_{zx} \\ -I_{xy} & I_{yy} & -I_{yz} \\ -I_{zx} & -I_{yz} & I_{zz} \end{bmatrix} \qquad (15)$$

All computations were done in the basic reference (X-Y-Z) coordinate system. The subscript i denotes an individual component and the subscript G denotes the total for a group. When spacecraft composite totals were calculated, G replaced i and the subscript T, denoting total, replaced G. n is the number of components in each group or the number of groups in the composite computations.

Pound (lb) units were used in calculating weight. Lb-in.^{2} units were used in calculating centroidal moments and products of inertia. These units are inconsistent with the definitions of mass moments and products of inertia. They were used purely for convenience, and no complications or confusion resulted. Before formation of the inertia matrix, a conversion to slug-ft^2 units was made.

B. Computer Program Utilization

A complete set of computer runs for each spacecraft configuration was generated monthly prior to launch and a summary of composite properties published. If a major design change occurred, a run was made immediately to determine if the change was allowable from the standpoint of weight and cg control. As component hardware was fabricated, weighed weights were substituted for calculated weights in the input. As components were assigned to a particular flight spacecraft, three sets of runs were made, one for each vehicle. Thus, by the time each craft was available for experimental weight and cg determination, a very accurate prediction of the inertial properties was available. As the analytical results were dependent only on the input for accuracy (computer round-off error being negligible), the experimentally determined weight and cg provided a check on the computer program.

C. Computer Program Accuracy

Two sources of error in the computer program guaranteed that the weight and cg output would be less accurate than the empirical determination: (1) the rounding off of the input weights, and (2) the fact that the motor was nominally positioned for purposes of computation at $\alpha = 0$ deg with no translation. With no mistakes in input, the final analytical weight and cg should have agreed with the measured values within 2 lb and 0.25 in., respectively. The moments and products of inertia calculated were sufficiently accurate for all predictions in which these properties were needed.

There were no direct operations by the spacecraft that depended upon measured values of the moments and products of inertia. Computer estimates were adequate for sizing gas jet openings and for autopilot gain and attitude control analyses. Therefore, these inertial properties were not measured, whereas weight and cg were.

V. EXPERIMENTAL WEIGHT AND CENTER-OF-GRAVITY DETERMINATION

Mariner Mars spacecraft and cg measurement consisted of two parts, each requiring two experimental setups. In one part, the weight and cg of the spacecraft less the propulsion system were measured. In the other part, these properties were determined for the propulsion system itself. Then a rotation and two translations of the propulsion system (as discussed in Section III) were calculated to align the thrust vector with the combined cg. With these adjustments known, the weight and cg of the composite vehicle were calculated.

Two complete tests were run on each spacecraft. The first test was performed just after the initial buildup of the spacecraft. The results of this test were used to position the motor. The second test was conducted just prior to launch at the ETR to measure the changes because of hardware replacement, so that the magnitude of the correcting vernier adjustments could be determined. If the second measurement gave a misalignment of the nominal thrust vector to the cg that was outside the allocated vernier adjustment capability, the propulsion system would have to be remounted on a spare substructure. A special drill fixture was provided to machine the substructure at ETR.

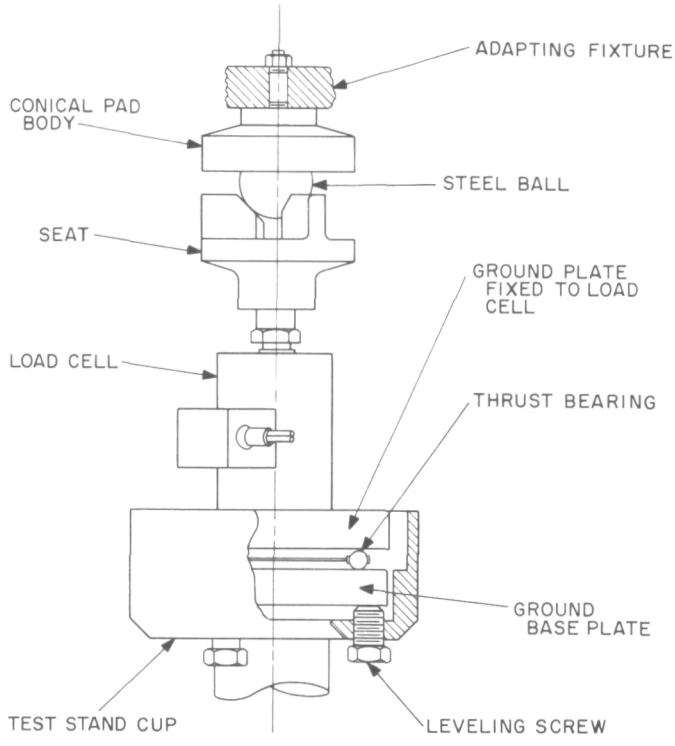


Fig. 13. Load cell installation

A. Center-of-Gravity Test Hardware

In all four setups of each complete test, reactions were measured by strain gage type compression load cells. Three cells were installed on the test stand in a triangular pattern. Figure 13 shows a load cell assembly. The load cell had a ground steel plate fixed to its base. This plate rested on a thrust bearing which sat on another ground steel plate. The base plate was leveled in the cup of the cg test stand. A steel seat was mounted to the top of the load cell. A ground steel ball was mounted in this seat. A pad with a conical bore was attached to the test adapting fixture which supported the spacecraft or motor assembly. The pad containing the conical bore rested on the ball. The rotational freedom allowed by the ball, plus the translational freedom gained by the thrust bearing, guaranteed that only axial loads would be transmitted through the load cell. This was necessary because any applied side load appreciably affected the accuracy of the load cell. The tops of the steel balls in each of the three assemblies were adjusted to be in a level plane before a test. The dimensional relationships of the load cells to one another were fixed by the dimensions of the adapting fixture holding the item to be weighed. To obtain the weight and cg of the spacecraft, 500-lb load cells were used. To obtain the weight and cg of the propulsion system, 100-lb cells were used. Each type of load cell had a manufacturer's guaranteed accuracy of $\pm 0.1\%$ of full scale or ± 0.5 and ± 0.1 lb, respectively. Reactions were recorded from a digital readout system to obtain high data resolution.

B. Measurements of the Spacecraft Less the Propulsion System

The two steps required to perform this part of the test are described separately.

1. Weight and Center of Gravity in the Plane of Bay II

The two coordinates of the cg in the plane of Bay II, u_s and v_s and the weight of the spacecraft were determined by this test. The setup is shown in Fig. 14. Because of geometric constraints, it was impossible to measure reactions by placing the spacecraft directly on the load cells. Hence, a fixture was required to adapt from the propulsion system mounting brackets in Bay II to the load

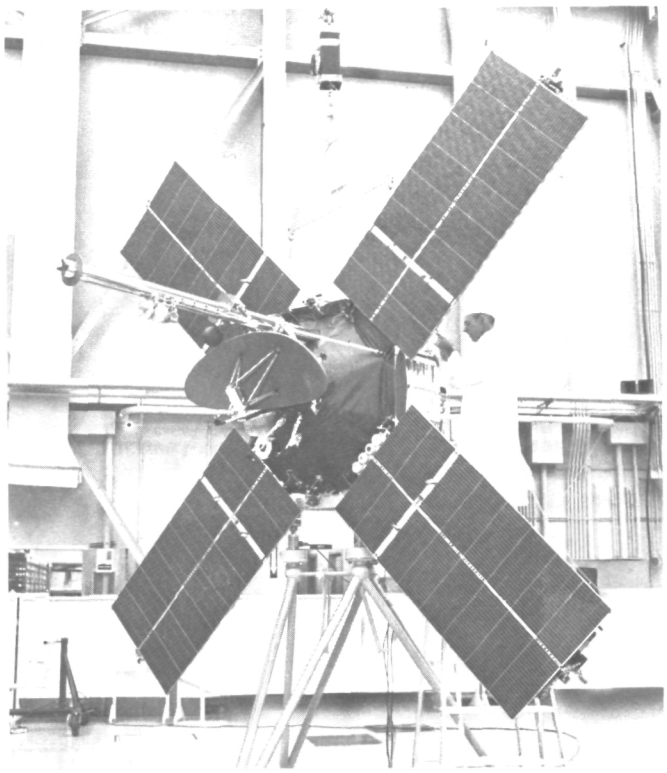


Fig. 14. Spacecraft center-of-gravity test in plane of Bay II

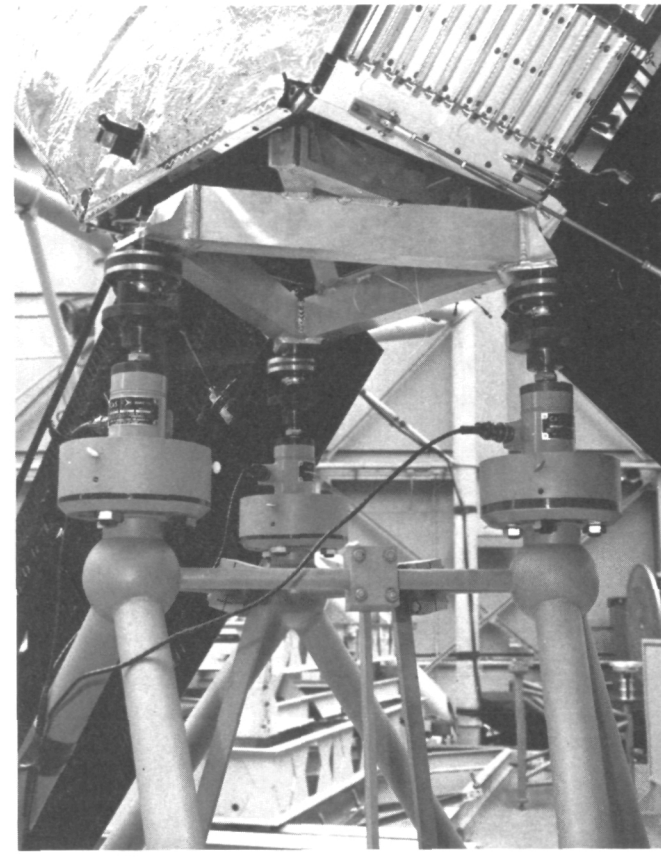


Fig. 15. Spacecraft-to-load cell adapter

cells. This fixture is shown in Fig. 15. It is essentially two triangles, one a right triangle that mounts to three of the four motor substructure/octagon mounting brackets, and the other an equilateral triangle whose apices located the 500-lb load cells.

The spacecraft, with the fixture installed, was set on the load cells as shown in Figs. 14 and 15. The solar panels were held open by struts, the lengths of which had been adjusted to hold the panels in a plane perpendicular to the roll axis. The solar vanes were folded. Reactions were recorded from the three load cells. The spacecraft was rotated 120 deg with respect to the load cells and readings recorded. The spacecraft was again rotated 120 deg and readings taken so that the average of the three readings taken at each point could be used to calculate the cg coordinates, u_s and v_s. This method minimized load cell and leveling errors.

Calculations of the projected position of the cg into the plane of Bay II was a simple statics problem. The example given here includes the determination of $\bar{v}_s$. The determination of $\bar{u}_s$ is done similarly. Figure 16 defines the dimensions used in the calculation of $\bar{v}_s$. R_0, R_1, and R_2 are the average measured reactions at points 0, 1, and 2. W_{F0}, W_{F1}, and W_{F2} are the previously measured reactions of the adapting fixture at the same three points. W_s is the weight of spacecraft. By summation of forces:

$$W_s = R_0 + R_1 + R_2 - (W_{F0} + W_{F1} + W_{F2}) \quad (16)$$

By taking moments about 0,

$$W_s(c + \bar{v}_s) + W_{F1}a + W_{F2}b = R_1a + R_2b$$

or

$$\bar{v}_s = \frac{(R_1 - W_{F1})a + (R_2 - W_{F2})b}{W_s} - c \quad (17)$$

Corrections for missing attitude-control gas, the struts supporting the solar panels, undeployed solar vanes, and other test and missing flight hardware had to be made on these values. These corrections were made using equations similar to Eqs. (11) and (12) but in the u-v-w coordinate system.

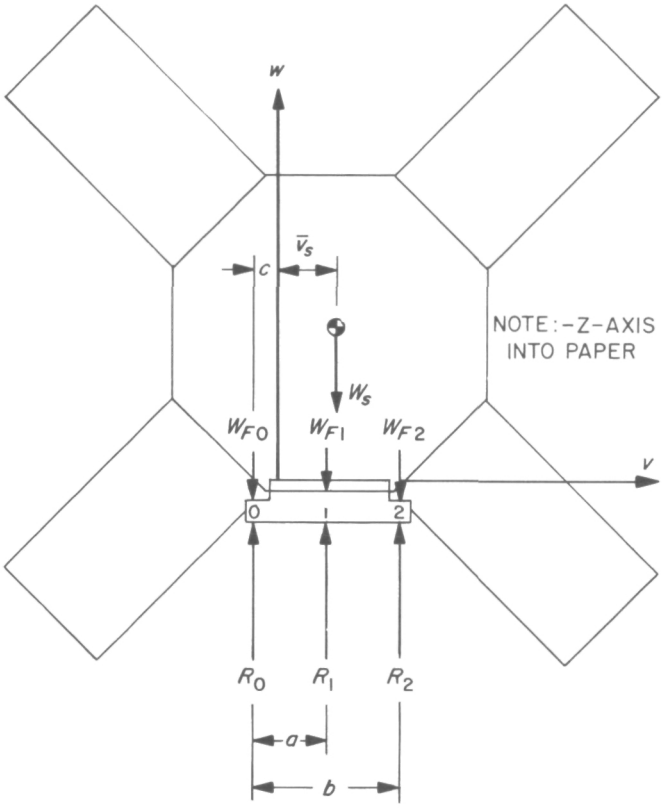


Fig. 16. Weights and reactions in center-of-gravity measurement

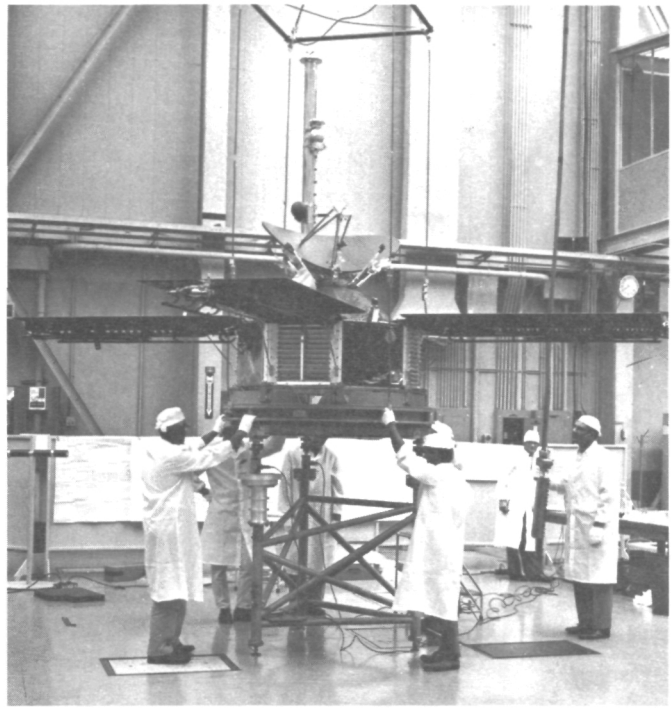


Fig. 17. Spacecraft center-of-gravity test normal to plane of Bay II

2. Center of Gravity Normal to the Plane of Bay II

The coordinate of the center of gravity of the spacecraft less the propulsion system normal to the plane of Bay II, $\overline{w}_s$, was obtained from this test. The setup is shown in Fig. 17. The spacecraft was mounted to a handling ring that had been fitted with a triangular adapter where apices located the load cells. This assembly rested on the three 500-lb load cells as shown in the photograph. Reactions were recorded at each point of the triangular adapter. The spacecraft was rotated 120 deg and the readings taken again. This process was repeated again until three sets of load cell readings had been recorded. Averaging the three sets of readings minimized load cell and leveling errors. Figure 18a shows the spacecraft in this orientation in which reactions R_2, R_5, and R_7 were measured, each subscript referring to the spacecraft bay number closest to the triangular apex measuring point. W_u was the unmeasured weight of the handling ring and triangular adapter and W_s was the spacecraft weight determined by Eq. (16) in the previous test. Taking moments about a line through points R_5 and R_7:

$$W_s(f - \overline{w}_s) + W_u d = R_2 e \tag{18}$$

The spacecraft was then rotated 180 deg with respect to the handling ring and the process repeated. This second orientation is shown in Fig. 18b. The position of the cg of the ring and adapter was not changed. Taking moments about the same line, this time labeled $R_1 - R_3$ because of the rotation of the spacecraft:

$$W_s(\overline{w}_s - g) + W_u d = R_6 e \tag{19}$$

Subtracting Eq. (18) from Eq. (19),

$$W_s(2\overline{w}_s - f - g) = (R_6 - R_2)\, e$$

or

$$\overline{w}_s = \frac{(R_6 - R_2)\, e}{2W_s} + \frac{(f + g)}{2} \tag{20}$$

Notice that the weight of the handling ring W_u and its cg position d, drop out of the calculation. This method, rather than measuring the weight and cg of the handling ring, was used to increase the accuracy and reduce the calibration time.

Using the other measured reactions by an identical method, a check was made on the v cg coordinate of the spacecraft, $\overline{v}_s$ obtained during the spacecraft cg test in to the plane of Bay II.

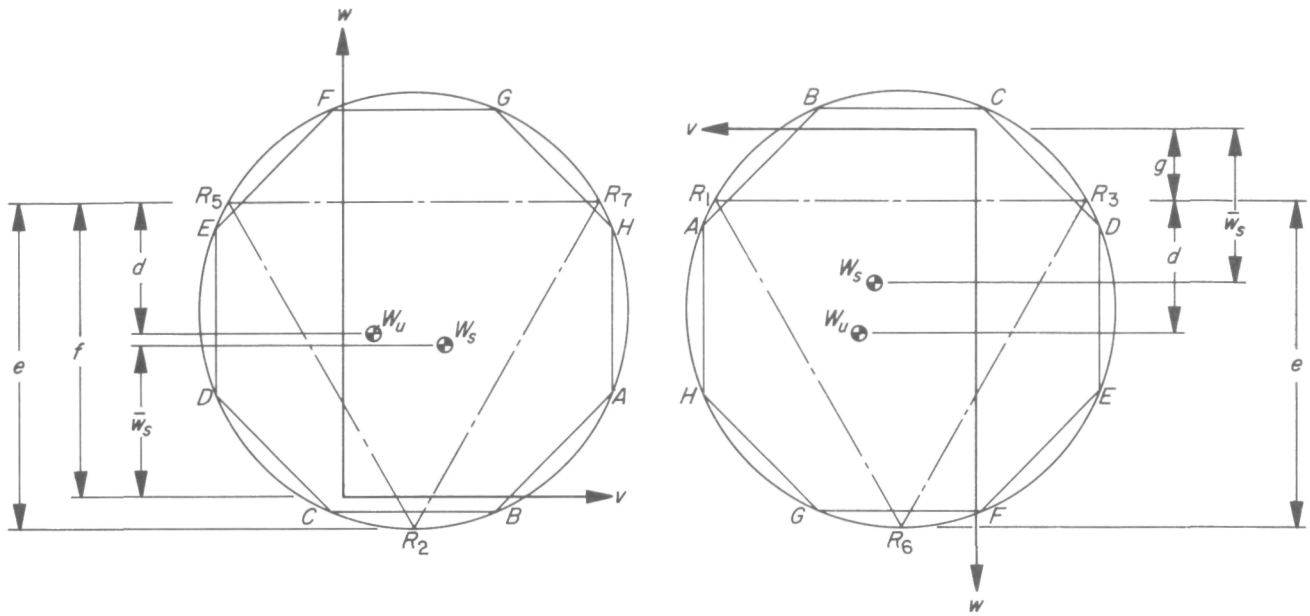


Fig. 18. Weights and reactions for determination of w_s

C. *Measurement of the Propulsion System*

The weight and cg of the propulsion system were measured before fueling. The propulsion system was mounted to a substructure with known rotation α and known translation Δv and Δu_a. For the initial test, α was a nominal 3 deg and the translations were zero, but for the final test just prior to launch, the positioning was that determined by the initial cg measurement. Two setups were required: one for the weight and cg as projected into the plane of Bay II, u_p and v_p; and one for the cg normal to the plane of Bay II, w_p. Figure 19 shows the first setup, and Fig. 20 shows the second. The propulsion system was mounted to the midcourse motor-weighing fixture. This fixture could be set on the three 100-lb load cells in two planes at right angles to each other as illustrated by the two photographs. The same stand used in the spacecraft Bay II cg test was used for both of these test setups. In each setup, three sets of reactions were taken with the motor in three positions relative to the load cells. The positions were 120 deg apart. This was done, as in the case of the spacecraft tests, to minimize load cell and leveling errors. From the average reactions and inspected dimensions of the weighing fixture, the weight and three coordinates of the cg were determined by equations similar to Eqs. (16) and (17). Corrections for the fixture were included in the calculations. Corrections for missing propellant and nitrogen gas and the mislocated cable harness, shown in Fig. 19, were also made.

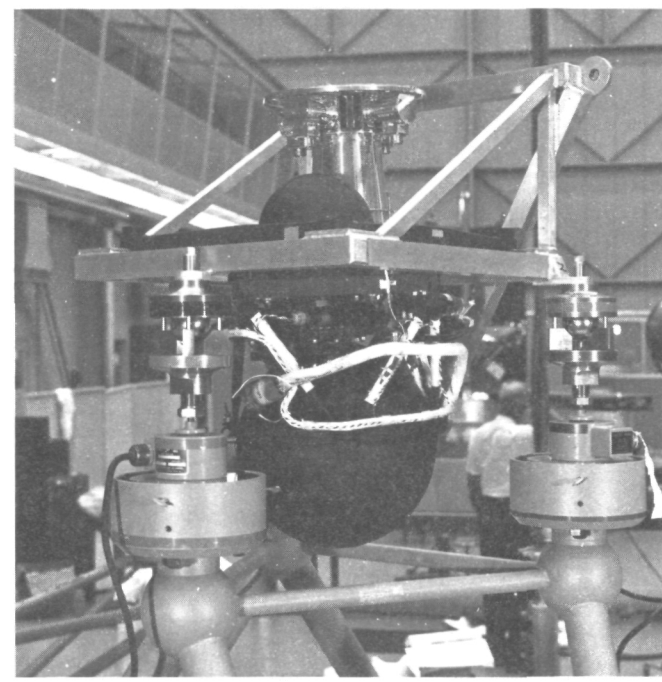


Fig. 19. Propulsion system center-of-gravity test in plane of Bay II

D. *Calculation of Alignment Adjustments*

Having measured the weights and centers of gravity of the spacecraft and the propulsion unit and made all necessary corrections on these parameters, the calculations

to correctly position the motor were made. The substructure weight was subtracted from the propulsion unit and added to the spacecraft. This was done because the substructure did not translate and rotate as the propulsion system was adjusted but was fixed to the spacecraft. Mathematical transference of the substructure was performed by equations similar to Eqs. (11) and (12). The following properties of the spacecraft and adjustable propulsion system were determined during the test:

W_s corrected spacecraft weight plus the substructure.

W_p corrected propulsion system weight minus the substructure.

$\bar{u}_s$, $\bar{v}_s$, $\bar{w}_s$ corrected coordinates of the cg of the spacecraft including the substructure.

$\bar{u}_p$, $\bar{v}_p$, $\bar{w}_p$ corrected coordinates of the cg of the propulsion system less the substructure in the position as measured.

The following dimensions also necessary in the adjustment calculations were known:

u_R, w_R coordinates of the spacecraft fixed motor pivot line.

α_0 the angle at which the motor was positioned during measurement. For the initial test, $\alpha_0 = 3$ deg as described in Subsection C.

v_T The v coordinate of the motor center line as positioned during measurement. This was the v coordinate of the center of Bay II plus any previously included translation, Δv_0, that resulted from the initial positioning.

$u_T - u_R$ The distance between the pivot line and the motor center line during measurement. This distance is the 2.000 in. illustrated in Fig. 8 plus any included translation, Δu_{α_0}, that resulted from initial positioning.

A rotation α and additional translations $\Delta v'$ and Δu_α to align the motor center line with the cg had to be determined. For the initial measurement α was not necessarily equal to α_0, but for the final measurement $\alpha = \alpha_0$. This is explained in the next Section. For the initial measurement, the motor was positioned so that Δu_{α_0} and Δv_0 were zero. Thus, Δu_α was equal to $\Delta u'_\alpha$ and Δv was equal to $\Delta v'$. For the final measurement by the definition illustrated in Fig. 9, Δu_α was the sum of Δu_{α_0} and $\Delta u'_\alpha$ and Δv was the sum of Δv_0 and $\Delta v'$.

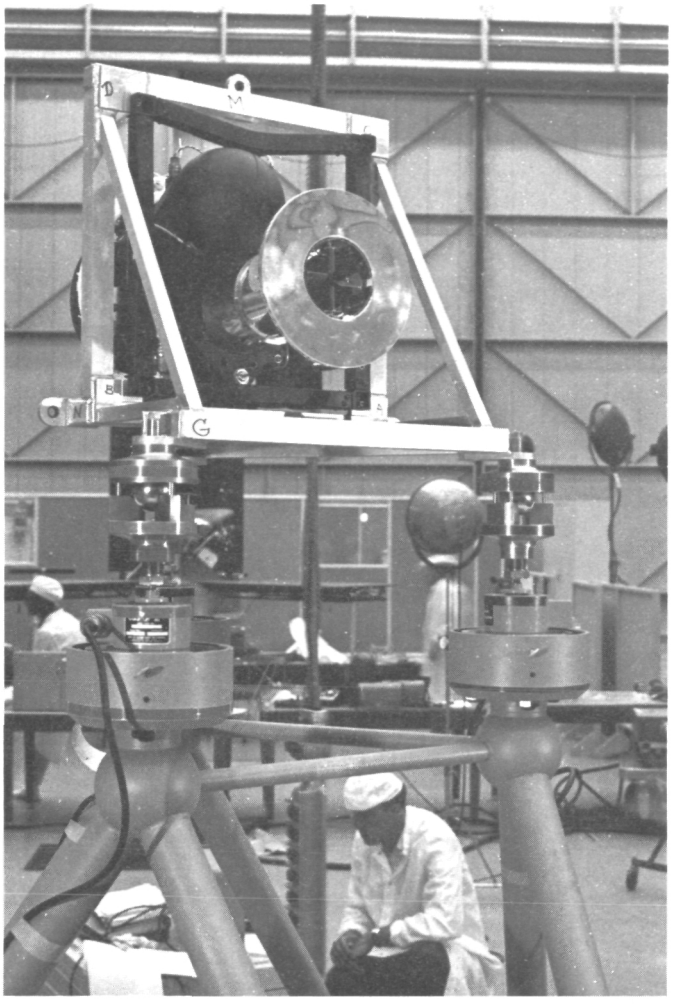


Fig. 20. Propulsion system center-of-gravity test normal to plane of Bay II

These dimensions are shown in Figs. 21 and 22, which will also serve to illustrate the development of the alignment equations. The calculation of Δv is described first as it was the simplest and will illustrate the method.

Figure 21 shows the dimensions necessary to determine Δv. Taking moments about the u axis,

$$W_p(\bar{v}_p + \Delta v') + W_s\bar{v}_s = (W_s + W_p)(v_T + \Delta v')$$

or

$$\Delta v' = \frac{W_p}{W_s}(\bar{v}_p - v_T) + (\bar{v}_s - v_T) \qquad (21)$$

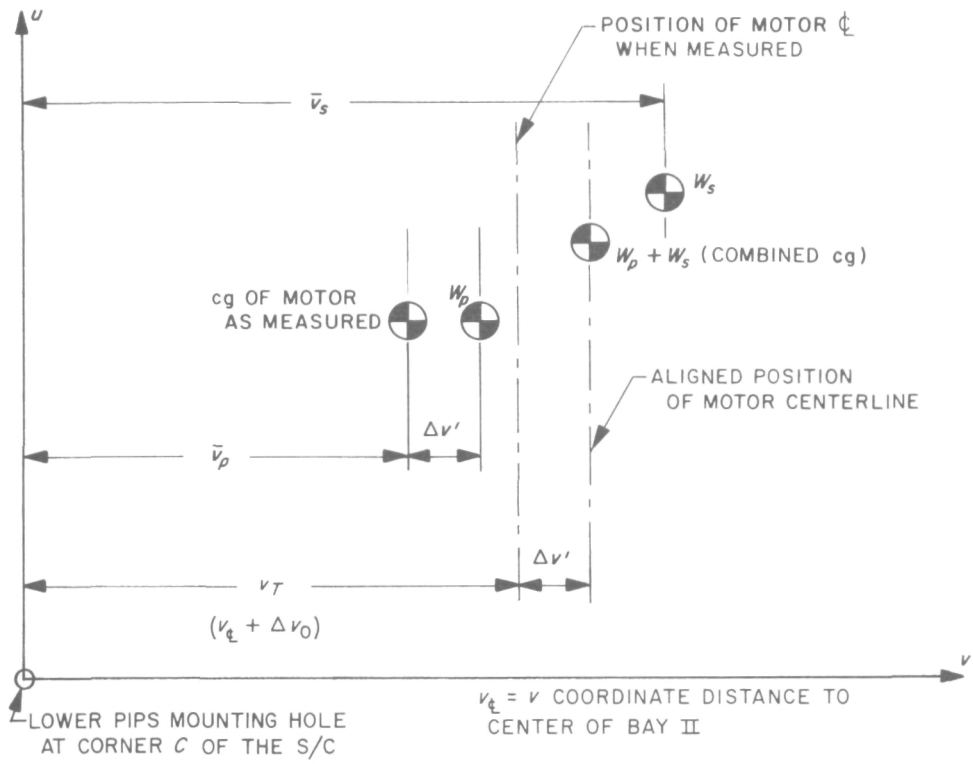


Fig. 21. Horizontal alignment of thrust vector and combined center of gravity

From the previous discussion, the following two equations may be written as:

$$\Delta v = \Delta v_0 + \Delta v'$$

$$v_T = v_{\ell} + \Delta v_0 \tag{23}$$

v_{ℓ} may be calculated directly from Eq. (3) by setting $X = Y$. Figure 22 shows the dimensions necessary to determine the redundant adjustments, rotation α and vertical translation $\Delta u'_{\alpha}$. When the weight and cg of the propulsion system were measured, the angle of rotation was α_0, and the line *R-B* in the figure was horizontal. When aligned, the angle of rotation was α as shown in the diagram. Taking moments about line *R-A*,

$$(k - h + \Delta u'_{\alpha}) W_p + (n - m) W_s = (u_T - u_R + \Delta u'_{\alpha}) (W_s + W_p)$$

substituting the definitions given in the figure:

$$[(\bar{u}_p - u_R) \cos \alpha_0 - (\bar{w}_p - w_R) \sin \alpha_0 + \Delta u'_{\alpha}] W_p + [(\bar{u}_s - u_R) \cos \alpha - (\bar{w}_s - w_R) \sin \alpha] W_s = (u_T - u_R + \Delta u'_{\alpha}) (W_s + W_p) \tag{24}$$

As previously discussed, the following two equations may be written:

$$\Delta u_{\alpha} = \Delta u_{\alpha_0} + \Delta u_{\alpha} \tag{25}$$

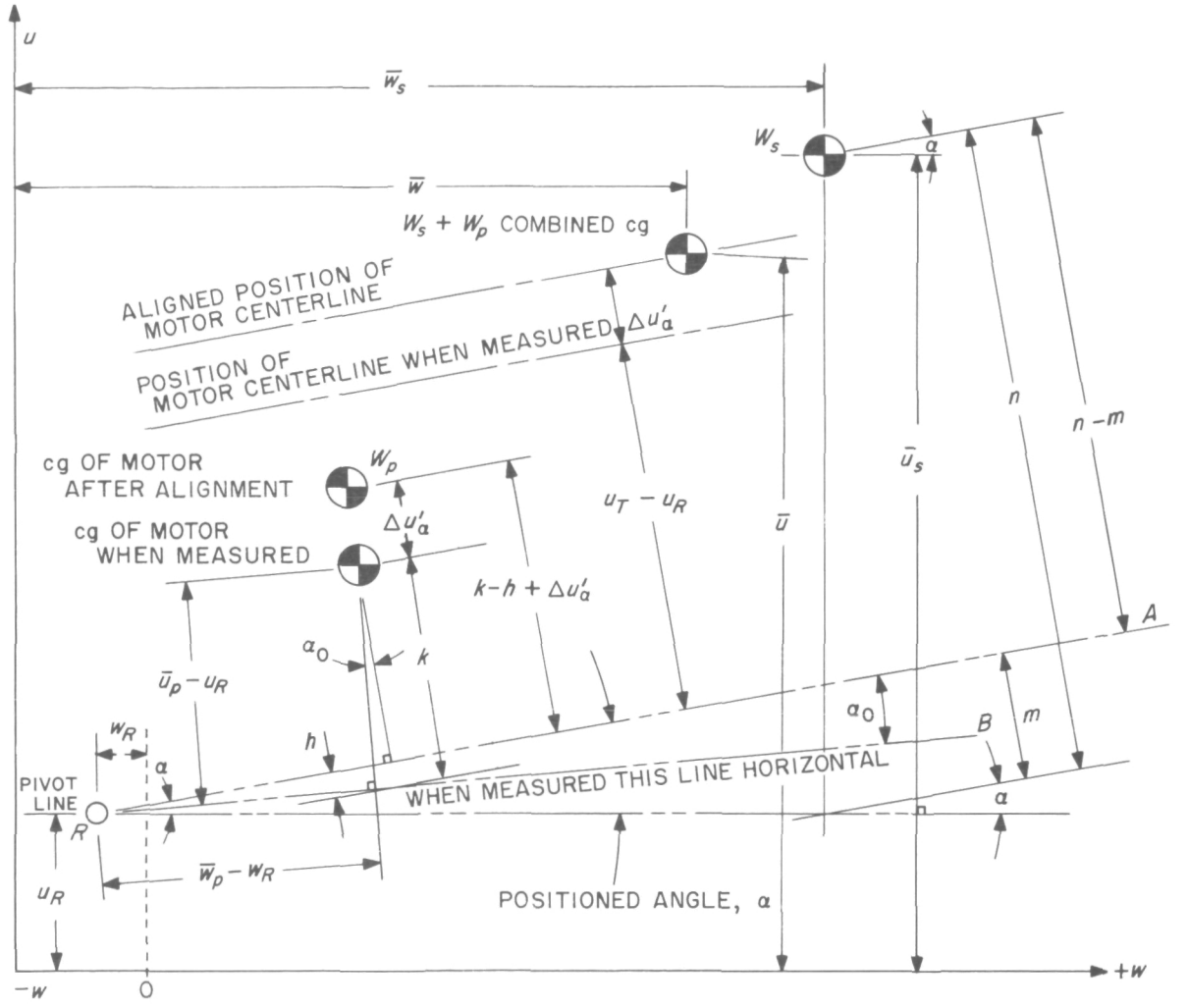
$$u_T - u_R = 2.000 \text{ in.} + \Delta u_{\alpha_0} \tag{26}$$

Equation (24) may be written in simpler form for each case in which it is used. First, consider the case of the initial cg measurement in which $\Delta u_{\alpha_0} = 0$. Thus, by Eq. (25):

$$\Delta u'_{\alpha} = \Delta u_{\alpha}$$

and by Eq. (26):

$$u_T - u_R = 2.000 \text{ in.}$$



α_0 = ANGLE OF ROTATION WHEN cg OF PROPULSION UNIT IS MEASURED

$h = (\bar{w}_p - w_R) \sin \alpha_0$ $\qquad u_R = 8.125$

$k = (\bar{u}_p - u_R) \cos \alpha_0$ $\qquad w_R = -0.665$

$m = (\bar{w}_s - w_R) \sin \alpha$ $\qquad u_T - u_R = 2.000 + \Delta u_{\alpha_0}$

$n = (\bar{u}_s - u_R) \cos \alpha$

Fig. 22. Vertical alignment of thrust vector and combined center of gravity

If α was not pre-established, it could be determined for the condition of no vertical translation by setting $\Delta u_\alpha = 0$ in Eq. (24). This yielded

$$(\bar{u}_s - u_R)\cos\alpha - (\bar{w}_s - w_R)\sin\alpha = 2 + \frac{W_p}{W_s}[2 - (\bar{u}_p - u_R)\cos\alpha_0 + (\bar{w}_p - w_R)\sin\alpha_0] \tag{27}$$

This is a transcendental equation for α, the only unknown. A graphical solution is appropriate. However, a good first approximation may be found by setting $\cos\alpha = 1$ and $\sin\alpha = \alpha$ as α was always less than 4 deg. If a particular α was desired, to make all rotations identical for instance, Eq. (24) was solved for Δu_α after the initial cg measurement. For this case, Eq. (24) took the form

$$\Delta u_\alpha = \frac{W_p}{W_s}\left[(\bar{u}_p - u_R)\cos\alpha_0 - (w_p - w_R)\sin\alpha_0\right] + (\bar{u}_s - u_R)\cos\alpha - (\bar{w}_s - w_R)\sin\alpha - 2\left(\frac{W_p}{W_s} + 1\right) \tag{28}$$

This equation could be solved directly for Δu_α when α was specified. Δu_α found here became Δu_{α_0} for the second measurement. In the case of the second measurement, α was automatically equal to α_0 as any readjustment of the alignment was performed by changing only the two translations. In this case, Eq. (24) became:

$$\Delta u'_\alpha = \frac{W_p}{W_s}[(\bar{u}_p - u_R)\cos\alpha - (w_p - w_R)\sin\alpha] + (\bar{u}_s - u_R)\cos\alpha - (\bar{w}_s - w_R)\sin\alpha - (2 + \Delta u_{\alpha_0})\left(\frac{W_p}{W_s} + 1\right) \tag{29}$$

As will be explained, the decision as to whether to reposition the motor after the final cg measurement was a function of the magnitude of the misalignment at that time. The two components of this misalignment were given directly by Eqs. (21 and 29). If the motors were not repositioned, these misalignments entered directly into vernier adjustment calculations.

E. Calculation of the Combined Center of Gravity

After determining the three adjustments necessary to align the motor's undeflected thrust axis with the composite cg, the position of the combined cg of the spacecraft and propulsion system was calculated. The three equations come directly from Figs. 21 and 22.

$$\bar{u} = \frac{W_s\bar{u}_s + W_p[\Delta u'_\alpha\cos\alpha + (\bar{u}_p - u_R)\cos(\alpha - \alpha_0) + (w_p - w_R)\sin(\alpha - \alpha_0) + u_R]}{W_s + W_p} \tag{30}$$

$$\bar{v} = \frac{W_s\bar{v}_s + W_p(\bar{v}_p + \Delta v')}{W_s + W_p}$$

$$\bar{w} = \frac{W_s\bar{w}_s + W_p[w_R + (\bar{w}_p - w_R)\cos(\alpha - \alpha_0) - (\bar{u}_p - u_R)\sin(\alpha - \alpha_0) - \Delta u'_\alpha\sin\alpha}{W_s + W_p} \tag{31}$$

The position of the measured cg in the basic reference (X-Y-Z) system could be determined by using the transformation given by Eq. (5).

After the initial measurement of the center of gravity on the first two flight spacecraft, a rotation of the propulsion system was chosen. The angle, α, was picked to allow both motors to have the same rotation.

A 2-deg angle was chosen, as it was less than ¼ deg from the results given for both spacecraft by Eq. (27). This integral angle allowed maximum vertical translations, and minimized the chances of machining errors.

VI. SUBSTRUCTURE MACHINING OPERATIONS

A. Substructure Machining Sequence

With α specified, Δu_α was calculated by Eq. (28). Δv was calculated by Eqs. (21)–(23) setting $v_T = v_{\mathfrak{L}}$. An appropriate set of midcourse mounting blocks were bolted to a substructure. The substructure was then mounted to the table of an optical setup jig bore with plane B set at 2 deg to the plane of the cutting tool. The tops of the four blocks were then cut co-planar so the finished plane C was 2.125 in. from the pivot line, shown in Fig. 9. The motor mounting-hole pattern was then drilled and reamed at the proper translations, Δv and Δu_α, without removing the substructure from the setup. The accuracy of the angle α was better than ± 1 min, and the accuracy of the hole locations relative to the reference substructure-to-spacecraft mounting holes (the u-v axis locators), was better than ± 0.001 in.

A spare substructure was assembled and plane C cut to the same angle. No holes were drilled in mounting blocks of this spare, however. It was shipped to the launch site with the spacecraft and was to be used if the shift in cg, determined by the final cg measurement, was outside the allocated vernier adjustment capability. The criteria for the use of the spare frame, as shown in the next Section, was that the vector sum of the distance from the cg to the prepositioned motor thrust axis at the time

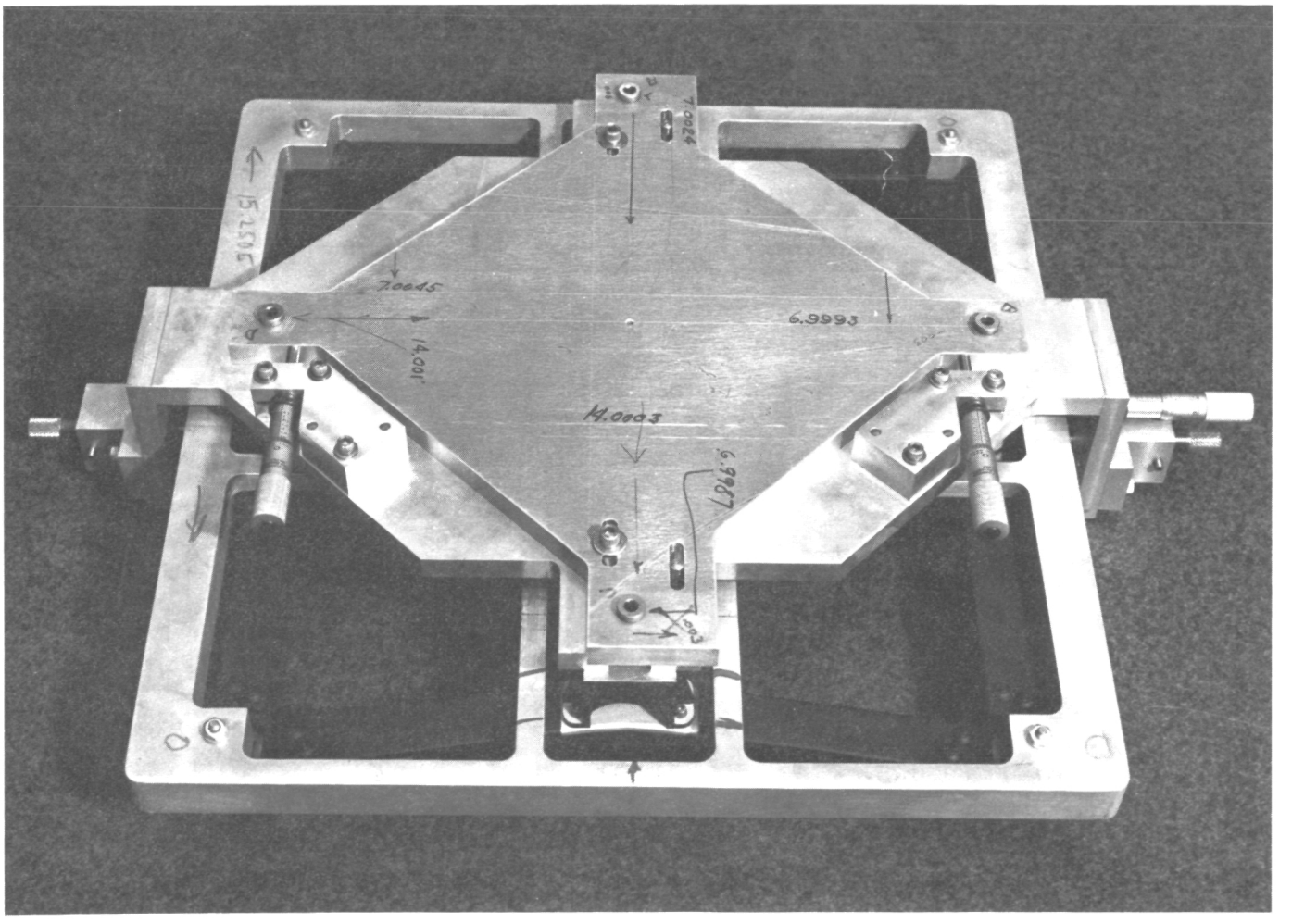


Fig. 23. Spare substructure drill jig

of the final cg measurement had to be greater than 0.125 in. In other words, if the following inequality was satisfied, the spare substructure would have been used.

$$[(\Delta u'_a)^2 + (\Delta v')^2]^{1/2} > 0.125$$

where $\Delta u'_a$ was calculated by Eq. (29) and $\Delta v'$ was calculated by Eq. (21) setting v_T equal to the value given in Eq. (23).

B. Spare Substructure Drill Fixture

As there was no machine at the launch site capable of accurately locating the motor mounting holes in the substructure, a special tool was designed and fabricated. This drill jig, designed for use with a hand-held drill motor, is shown in Fig. 23. The drill jig consisted of a frame and two movable plates. If it was necessary to use the jig at the ETR, the spare substructure could have been installed in the jig frame as shown. One plate was mounted to the frame by a hinge that allowed the plate to rotate and translate parallel to the axis of rotation. With the substructure in place, the plate rested directly on the machined blocks that mounted the motor; thus, the angular rotation of the plate was set to conform with the substructure. The translation which was equivalent to the adjustment Δv, was set by the single micrometer at the side of the tool. The second plate was mounted to the lower plate by pins in guide slots. The third adjustment, Δu_a, was obtained by translating the top plate relative to the base plate by means of the two micrometers shown. The top plate held four hardened steel bushings in a pattern equivalent to the hole pattern of the motor thrust plate. These bushings were the guides for the drilling operation.

The misalignment at the time of final cg measurement was within the allocated vernier adjustment capability, eliminating the need for using the spare substructure.

VII. METHOD OF VERNIER ADJUSTMENTS

A. Schematic Description

Modifications to spacecraft turns could be made during the midcourse maneuver to correct for a known misalignment between the undeflected thrust vector, or motor centerline, and the actual cg. This method, by which these corrections are made, is called the method of vernier adjustments. Figure 24 is a simplified schematic diagram of the midcourse maneuver; Part I shows what would happen during the maneuver if no corrections were made, and Part II illustrates how a vernier adjustment on the turn would correct for the misalignment and consequent pointing error. Figure 24a shows the premaneuver spacecraft orientation, and 24b the direction of the desired velocity increment that was needed to correct the spacecraft's trajectory. Figure 24c shows the orientation of the spacecraft after the maneuver turn, but before motor ignition. It was on this turn (actually two successive turns by the *Mariner* Mars) that the vernier adjustment could be applied to correct for misalignments. All successive steps of the maneuver were identical for an uncorrected or corrected maneuver. As shown in Fig. 24d, when the motor ignited, the thrust vector was initially along the motor center line. This caused a torque about the cg that rotated the spacecraft. This rotation was terminated when the spacecraft's autopilot nulled the spacecraft rotational velocities. The autopilot converted the error signals from the gyros into appropriate position commands for the jet vanes, which, in turn, deflected the thrust vector so that it found a stable condition in which the orientation of the spacecraft remained fixed. Figure 24e shows the condition in which the stabilized thrust vector pointed directly through the cg. Neglecting initial transient thrust in a different direction, the direction of the stabilized thrust vector in inertial space was the same as the direction of the actual velocity increment imparted to the spacecraft.

B. Vernier Adjustment Calculations

1. General

The angle between the velocity increments, Δv actual, in the corrected and uncorrected maneuvers illustrated

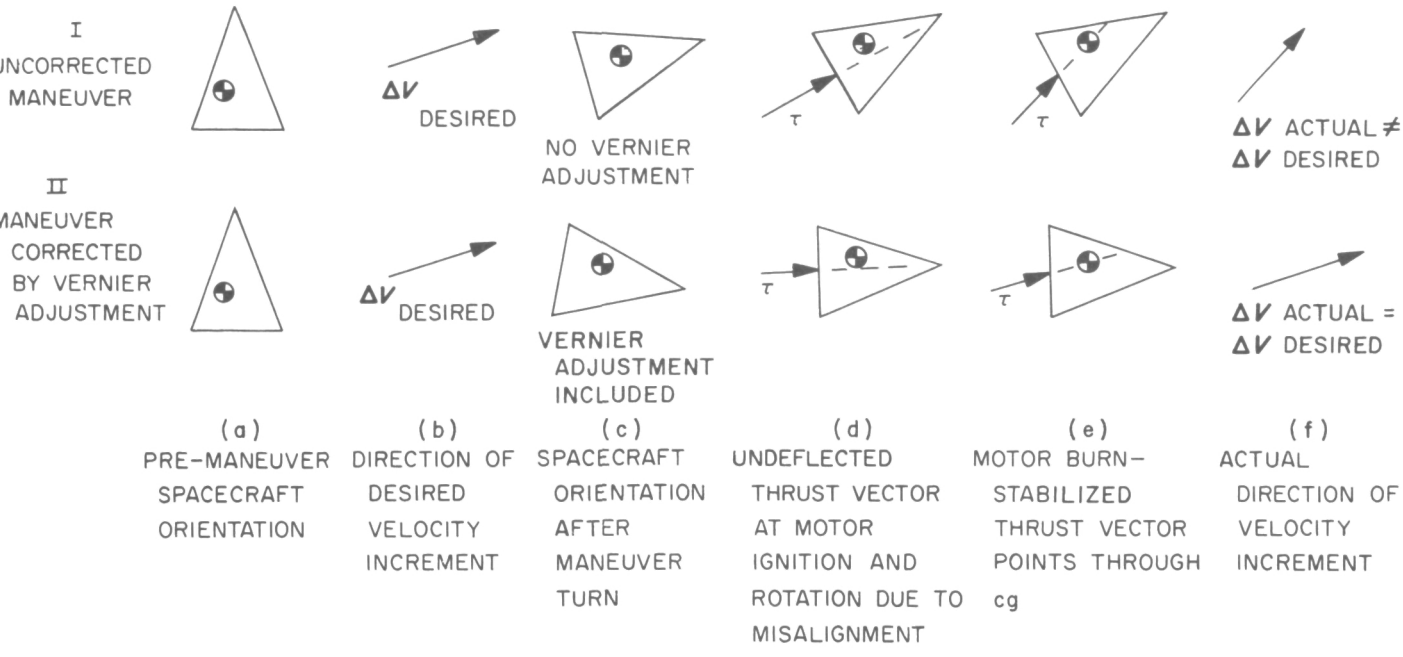


Fig. 24. Midcourse maneuver schematic

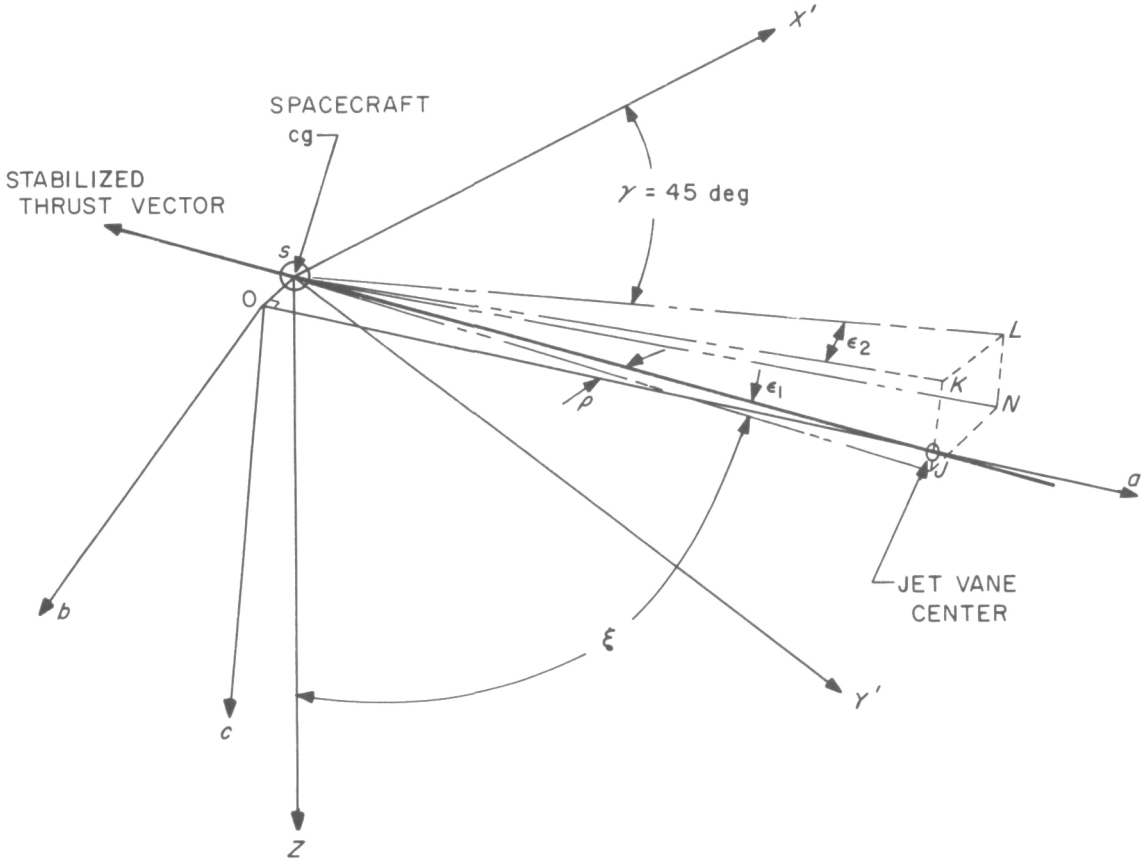


Fig. 25. Stabilized thrust vector

in Fig. 24f was the vernier adjustment angle applied to the turn of Fig. 24c for the corrected maneuver. This angle was composed of the actual angular misalignment of the undeflected thrust vector and cg plus the initial transient rotations because of this misalignment. Two calculations were necessary to determine the total angle, which was the vernier adjustment, and both were mechanized into one computer program. Before discussing this program, it is necessary to describe the transformations that were necessary to calculate the angular misalignments of the undeflected thrust vector and the stabilized thrust vector.

Figure 25 shows the steady state, or stabilized thrust vector, and the geometrical angular misalignments. The a-b-c and X'-Y'-Z' axes were as shown in Fig. 7. The stabilized thrust vector passed through the jet vane center of lift and the spacecraft center of mass. The projection of the stabilized thrust vector in the X'-Y' plane, SK, made an angle of $\gamma + \varepsilon_2$ to the X' or pitch axis. γ was 45 deg because of motor positioning constraints. The thrust vector made an angle of $\xi + \varepsilon_1$ to the Z' or roll axis. ξ was the complement of α and was between 86 and 90 deg. Angles ε_1 and ε_2 were positive as shown. These angles did not define the complete magnitude of the vernier adjustments, only the geometrical offset of the thrust axis from the cg.

The direction cosines of the steady state thrust vector in the X'-Y'-Z' coordinate system were:

$$SJ \left| \begin{array}{c|c|c} X' & Y' & Z' \\ \hline \cos(45\text{ deg} + \varepsilon_2)\sin(\xi + \varepsilon_1) & \cos(45\text{ deg} - \varepsilon_2)\sin(\xi + \varepsilon_1) & \cos(\xi + \varepsilon_1) \end{array} \right.$$

Angle ε_1 can be expressed in terms of the X', Y', and Z' coordinates of the jet vane center as:

$$\varepsilon_1 = \arctan\left[\frac{[(X'_J)^2 + (Y'_J)^2]^{1/2}}{Z'_J}\right] - \xi \tag{33}$$

or in terms of the a, b, and c coordinates of the cg and jet vane center of lift as

$$\varepsilon_1 = \arctan\left[\frac{(a_J^2 \sin^2\xi + c^2\cos^2\xi + b^2 + 2a_J c\cos\xi\sin\xi)^{1/2}}{a_J\cos\xi - c\sin\xi}\right] - \xi \tag{34}$$

If the average cg during midcourse was precisely at the position determined by the final cg measurement, then:

$$\bar{b} = -\Delta v'$$

$$\bar{c} = -\Delta u'_\alpha$$

This was not encountered because some hardware was replaced after the final cg measurement, and the average cg position during motor burn had to include the shift in cg due to midcourse fuel depletion.

Angle ε_2 was expressed in terms of the X', Y', and Z' coordinates of the jet vane center as

$$\varepsilon_2 = \arctan\left(\frac{Y'_J}{X'_J}\right) - 45\text{ deg} \tag{35}$$

or in terms of the a, b, and c coordinates of the cg and the jet vane center as

$$\varepsilon_2 = \arctan\frac{-\bar{b}}{a_J\sin\xi + \bar{c}\cos\xi} \tag{36}$$

Angle ρ, between the motor center line and the steady state thrust vector, was expressed in terms of ε_1 and ε_2 as

$$\cos\rho = \cos\varepsilon_1(\cos^2\xi + \cos\varepsilon_2\sin^2\xi) - \sin\varepsilon_1\sin\xi\cos\xi(1 - \cos\varepsilon_2) \tag{37}$$

Angle ρ could also be expressed in terms of the a-b-c system as

$$\cos\rho = \frac{a_J}{(a_J^2 + \bar{b}^2 + \bar{c}^2)^{1/2}} \tag{38}$$

Values of ε_1 and ε_2 did not define the complete magnitude of the vernier adjustments, only the geometrical offsets. The total angular offset, ρ, was the angle which had to be compared to the vernier adjustment capability. The vernier adjustment capability was the 20-mrad autopilot correction capability, minus the sum of possible errors and uncertainties in motor alignment procedure. The actual vernier adjustments were increased over the geometrical offsets by about 50% to account for the initial rotation of the spacecraft. These adjustments were not made in the spherical polar coordinate system describing ξ and γ, however, because of the requirement for a pitch turn followed by a roll turn.

2. Midcourse Maneuver Calculation Programs

The midcourse maneuver program computed maneuver pitch and roll turns, as well as burn time. One of the inputs to this program was the position of the thrust vector relative to the spacecraft as defined by the polar angles γ and ξ. If the polar angles were specified so that they include the geometrical offset and the additional transient rotation angles, the midcourse maneuver program automatically calculated the modified pitch and roll turns which corrected for the offsets. The polar angles to be specified in the final calculation were called ξ' and γ', so that

$$\xi' = \xi + \varepsilon_1 + \tau_1$$

$$\gamma' = \gamma + \varepsilon_2 + \tau_2$$

where ξ and γ were the polar angles that defined the position of the motor centerline and ε_1 and ε_2 were the respective geometrical offsets discussed before. Values τ_1 and τ_2 were the respective additional rotations of the spacecraft due to offset torques at motor ignition.

A separate digital computer program computed ξ' and γ'. Input to this program were the positions of the average cg and the jet vane center of lift in spacecraft reference coordinates, and the autopilot transfer function, a full 3 by 3 matrix, about the autopilot control axes, *a*, *b*, and *c*. First the computer found the radius vector, $\mathbf{R}_1$, from the cg to the jet vane center in the *a-b-c* system. Next the initial disturbance torque was computed by the equation $\mathbf{T} = \mathbf{R} \times \mathbf{F}_0$ where $\mathbf{F}_0$ was the known initial thrust vector. The rotation of the spacecraft about each axis was then computed as the inverse of the autopilot transfer matrix times the disturbance torque vector. A matrix was generated that defined the rotation of the *a-b-c* coordinate system due to the disturbance torque. The final stabilized thrust vector was along $-\mathbf{R}$. Using the rotation matrix, the final position of $\mathbf{R}$ was calculated in the autopilot coordinate system as oriented prior to motor ignition, and the angles ξ' and γ' computed.

The final calculation of ξ' and γ' used average position of the cg during motor burn. The burn time, and consequently the mass of the fuel to be used were found in a preliminary calculation by the midcourse maneuver program into which the *nominal* ξ and γ were the inputs. The cg shift due to half this fuel depletion was calculated, and the cg position appropriately modified. Also included in modifications to the cg position were shifts due to hardware replacement after final measurement, known attitude control gas depletion, and known postlaunch anomalies in the position of spacecraft articulating parts.

C. Magnitude of Vernier Adjustments

The preceding discussion illustrates some of the possible sources of cg shifts that were considered in calculating the magnitudes of the vernier adjustments. To determine the portion of the capability that could be reserved to account for cg shift due to hardware replacement between initial and final cg measurements, all possible uncertainties and possible cg shifts between the final cg measurement and the midcourse maneuver were subtracted from the autopilot correction capability. If the shift in cg between the two cg determinations were less than the remaining vernier adjustment capability, the spare substructure did not have to be drilled and used.

The autopilot had the capability of correcting for an offset in excess of 20 mrad. (The angle referred to is the amount the thrust vector had to shift to pass through the center of gravity.) To determine vernier adjustment capability, the sum of errors and uncertainties were subtracted from the autopilot's 20-mrad capability. Uncertainties considered were mechanical misalignments in the propulsion system assembly, concentricity of the undeflected thrust vector with the motor nozzle center line, cg measurement uncertainties, and unknown cg shifts due to attitude control gas depletion and deployed solar panel mislocation. Subtracting the 4.11-mrad 3σ sum of these uncertainties from the autopilot capability, it was determined that the method of vernier adjustments could be used to correct for offsets up to 15.89 mrad.

The portion of the vernier adjustment capability allocated for cg shifts after final cg measurement (which was

the final repositioning opportunity) was determined by considering possible shifts from three sources:

1. Hardware replacement after final cg measurement: To reserve vernier adjustment capability for this source of misalignment, a possible, but unlikely, set of circumstances was arbitrarily selected. These were exchanging two solar panels that differ in weight by ½ lb and a 3¼-lb addition or removal in the electronic cases. These changes would additively shift the cg by 6.84 mrad.

2. Possible failures: Three otherwise non-catastrophic failures were considered: (1) ninety percent attitude control gas depletion, (2) a solar vane failing to open, and (3) the science cover, which protects the TV camera, opening prior to the maneuver. These would cause a resultant maximum cg shift of 2.13 mrad.

3. Midcourse fuel depletion: for a second maneuver, 95% fuel depletion during the first maneuver was assumed. This would cause a 2.59-mrad cg shift.

Subtracting the sum of possible known misalignments due to the above three sources from the total vernier adjustment capability (15.89 − 6.84 − 2.13 − 2.59) gave a 4.33-mrad remainder. This amounted to a 0.125-in. shift of the cg at the roll axis. This, then, was the portion of the vernier adjustment capability allocated to account for cg shifts between initial and final cg measurements. It is this calculation that determined the inequality given in Section VI.

VIII. ACCURACY

The total midcourse maneuver accuracy of the *Mariner* Mars spacecraft was dependent upon the accuracies of many parameters. Two broad categories of independent error sources contributed to the accuracy of the pass by the planet. These were maneuver execution errors and orbit determination errors. Based on a priori knowledge before launch, approximately three-quarters of the uncertainties at Mars encounter were attributed to the maneuver execution errors.

The midcourse execution errors, with which this Report is concerned, were of two types, velocity-magnitude and pointing errors.

A. Velocity-Magnitude Errors

Velocity-magnitude errors were either proportional to or independent of the magnitude of the velocity increment. A thrust magnitude error was an example of an error source that is proportional to velocity. Examples of error sources independent of velocity, called velocity resolution error sources, were errors in ignition delay time, shut-off time, and thrust tail off.

B. Pointing Errors

Pointing errors arose because of the incorrect orientation of the thrust vector in inertial space during motor burn. The majority of the midcourse execution errors fell into this category, and contributed about 70% of the total. Some of these errors were dependent on the magnitude of the maneuver because they were proportional to the turn times. Sources contributing to the pointing error were misalignment and drift of the three gyros, spacecraft position in the attitude control rotational limit cycles, gyro rate calibration errors (which were strongly dependent on the gyro case temperature), mechanical misalignments of celestial body sensors, misalignments within the motor assembly, motor positioning errors, and cg determination errors.

The detailed contributions of the latter two errors are discussed below.

1. Center-of-Gravity Measurement Errors

The error in the weight and cg measurement was determined from the standard deviations of all possible errors within the measurement. The major source of error was load cell measurement uncertainty. This error was composed of the rms of the calibration error, plus the rms of the dispersion of actual measured reactions at any one point on any one spacecraft. Other sources of error were the inaccuracies in the measurement of fixture dimensions. Calibration errors of ±0.1 lb for the 500-lb load cells and of ±0.05 lb for the 100-lb cells were determined during load cell calibration. The standard deviation of the load

cell dispersions on spacecraft weighings was 0.36 lb, and on propulsion system weighings, σ was 0.09 lb. The measurement inaccuracy of fixture dimensions was figured as ± 0.0005 in. Taking the root-sum-square of all weighing errors gave a standard deviation of the spacecraft weight measurement of 0.42 lb. This number was then increased by 10% to account for errors in corrections to the final measured weights. The estimate on the standard deviation of the reported value of the final spacecraft weight was therefore $\sigma_E = 0.46$ lb.

To determine the 1σ uncertainty in the measured position of the cg, the total differential of each expression used in the calculation of the cg position was taken, and evaluated for the error using additive tolerances. This method is admittedly extremely conservative. The results indicated the cg had been determined within 0.050 in. As this result was an absolute tolerance, the standard deviation is this tolerance divided by root three, or $\sigma_E = 0.029$ in.

2. Midcourse Motor-Alignment Errors

Errors in midcourse motor alignment were from sources both considered and not considered in other sections of this Report. The error sources of interest were the accuracy of the positioning angles, and the accuracy of the relative location of the two hole patterns in the substructure. These were equivalently the accuracies of the machining of the angle α and of the hole pattern determined by Δu_α and Δv. As discussed in Section III, α had a tolerance of ± 1 min, or ± 0.29 mrad, and the tolerance on Δu_α and Δv was ± 0.005 in. Other errors in motor alignment were due to mechanical tolerances within the assembly of the propulsion system. All of these errors entered into the calculation of the 4.11-mrad 3σ uncertainty or thrust vector to cg alignment considered in the discussion of vernier adjustment capability in the last section.

C. Effects on Total-Maneuver Execution Accuracy

It is of interest to examine how these errors affected the total midcourse execution accuracy. The standard deviation of the final value of spacecraft weight caused a velocity magnitude error. For the average maneuver, this $\sigma_E = 0.46$ lb caused a ¼% contribution to the maneuver execution error. All other errors considered were of the pointing error type. The 1σ uncertainty of cg position, 0.029 in., caused a ½% contribution to the maneuver errors. All errors in mechanical alignments in the substructure and the motor, which included the tolerance on the angle α and the translations Δu_α and Δv, contributed another ¼% to the maneuver errors. Thus, the total error from the midcourse alignment and weight and cg measurement was only 1% of the total midcourse execution error. For comparison, the single error source from the roll gyro rate calibration contributed 22% of the total maneuver execution error.

IX. DISCUSSION AND RECOMMENDATIONS

This Report has described the experimental and analytical methods that were developed to determine the weight and cg of the *Mariner* Mars spacecraft. It has also described the methods used in alignment of the midcourse motor, and methods of maneuver correction for known misalignment between the nominal thrust vector and the cg. Center of gravity determination for the *Mariner* Mars was more complex than for previous JPL spacecraft. This was due to the positioning of the motor approximately perpendicular to the roll axis. However, the approach was as simple as was consistent with the geometrical constraints imposed and the accuracy required. *Mariner* Mars was the first JPL spacecraft to use rotational adjustments for propulsion system alignment. The accuracy with which these operations were performed resulted in very small contributions to total possible midcourse execution errors, and was the result of detailed consideration of all parameters. The most significant advances resulting from this portion of the *Mariner* Mars program were the further refinement of measurement and alignment methods and the development of the method of vernier adjustments.

A. Results of Interest

The weights measured by five tests on the three flight spacecraft manufactured varied from 574.27 to 575.62 lb. (The final measurement on the spare vehicle was not completed at the launch site because of the successful

launch of *Mariner IV*.) The location of the cg of each vehicle as measured in the same five tests did not vary more than 0.080 in. The small magnitudes of the ranges of weights and cg position indicate the consistency with which the spacecraft components were manufactured. The shifts between initial and final measurement, since they were less than 0.125 in., did not require motor repositioning at the ETR prior to the launch of *Mariner III* or *IV*.

The magnitude of the undeflected thrust vector to cg misalignment at launch was 0.022 in. for *Mariner III* and 0.010 in. for *Mariner IV*. At midcourse, the average position of *Mariner IV*s cg was misaligned 0.012 in., as determined by shifts due to half the known fuel depletion, and the abnormally high position of the four solar vanes. This amounted to 0.43-mrad angular offset, which was extremely small compared to the 15.89-mrad correction capability of the method of vernier adjustments. The corrected angles, ξ' and γ' were included in the input to the final maneuver calculation, but the corrections were too small to change the pitch and roll turn times that had been previously calculated.

B. Recommendations

Although the center of gravity measurement and motor alignment operations were very successful, as illustrated by the preciseness of the midcourse maneuver on *Mariner IV*, several problems arose during the program. Problems were either minor or solved, but their occurrence leads to the following recommendations for future programs.

1. Early in the preliminary mechanical design of a spacecraft, the method of measuring weight and cg and of adjusting the motor should be thoroughly considered. In the *Mariner* Mars 1964 program the design of the propulsion system's thrust plate had been frozen before the mounting and adjustment methods were chosen. Although a satisfactory substructure design evolved, mounting the motor directly to the spacecraft could have resulted in a lighter weight structure.

2. An extensive study to determine the constraints which limit the adjustment capability of the motor should be done early in a program. The adjustment capability determines the nominal cg envelope which should be as large as possible. The substructure flown on *Mariner* Mars was a second generation design. Its adjustment capability was approximately double that of the original design. No other changes had to be made to increase the capability, as the additional translational space already existed. The substructure re-design was required because analytical cg determinations showed that the cg fell outside the adjustment capability of the first substructure.

3. A conservative vernier adjustment capability should be estimated early to increase the allowable cg envelope and to determine the magnitude of allowable offsets. The method of vernier adjustments was developed late in the *Mariner* Mars 1964 program, primarily because the original functional requirement, which required that the cg be within 10 mrad of the motor centerline, was too restrictive and could not account for all possible shifts and errors. The method of vernier adjustments in this program was used in lieu of ballasting the spacecraft or realigning the motor just prior to launch. Because corrections could be applied directly to the maneuver turns for known offsets, the accuracy of the maneuver could be increased and the functional requirement restrictions relaxed. It is recommended that the maneuver turn adjustment capability be recognized early in the design and used.

4. Operational considerations, such as the desirability of minimizing last minute field operations, affected the motor alignment philosophy. The new method of vernier adjustments on maneuver turns, to correct for known thrust vector misalignment, potentially eliminated the need for repositioning the motor. Yet the philosophy remained simple, and the mechanization of weight and cg measurement and motor alignment was as crude as it was consistent with the requirements. This total approach is recommended.